A 2D exact model with stretching-through-the-thickness variable kinematic for the 3D exact analysis of laminated composite structures.

Arno Roland Ngatcha, J R Ngouanom Gnidakouong

A 2D exact model with stretching-through-the-thickness variable kinematic for the 3D exact analysis of laminated composite structures.

Arno Roland Ngatcha Ndengna[a,*], J.R. Ngouanom Gnidakouong[b]

[a]*Department of Maritime and Port Engineering, Laboratory of Energy Modeling, Materials and Methods, National Higher Polytechnic School of Douala ,University of Douala, P.O.BOX: 2107 Douala, Cameroon*
[b]*Department of Automotive and Mechatronic Engineering, Laboratory of Energy Modeling, Materials and Methods, National Higher Polytechnic School of Douala ,University of Douala, P.O.BOX: 2107 Douala, Cameroon*

Abstract

In this work, we introduce a novel 3D exact model for the analysis of the transient mechanical behavior of laminated composite plates and shells. The system of equations obtained by using Hamilton's principle, and the generalized ABCDE-matrix that accounts several essential mechanical couplings (due to variation in the thickness and section warping) often neglected in the classical literature. The stretching-through-the-thickness term is rigorously justified by the existence of potential of distortion proved here. It's found important to develop rigorously 3D exact analysis of mechanical behavior to improve the quality and resistance of laminated plate and shell structures for variety of applications. The proposed equations are assessed to show the performance of some matrix systems developed here in some selected test cases found in the literature. The 3D exact analysis proposed in the current work, improves many recent studies on the analysis of laminated composite plates and shells. Moreover, the generalized ABCDE-matrix has a great potential to increase the predicting power of the mechanical behavior of civil structures and the accuracy of analysis meanwhile reducing the computational costs.

Keywords: Laminated Shell models, stretching-through-the-thickness, 3D laminated constitutive relation, Exact laminated shell model, 3D exact analysis, Simple modified conventional algorithm.

1 Introduction

Great industrial efforts are made to improve the quality, durability and resistance of laminated shell structures (or composite materials with natural fiber reinforced) for variety of applications (including marine engineering, aerospace, hydraulic design among the others). A review on the tensile properties of natural fiber reinforced polymer composites [**?**]. For that, some theories or models have been developed to maximize the accuracy of analysis meanwhile reducing the computational costs. The static and dynamic of mechanical behavior of LCS can be difficult to analyze in practice due to several problems as anisotropy, nonlinearities, mechanical couplings, complex phenomena such as variation in thickness during the deformation that creates the transverse shear stress, the twisting along the normal axe that produces the membrane distortion in each section located at $-\frac{h}{2} \leq z \leq \frac{h}{2}$ and even the section warping. To solve all these problems, a complete exact model accounting the variation in thickness is required. Most of the models used or applied in engineering are heuristic adaptation of theory of thin shell of Kirchhoff-Love(K-L) where the classical displacement is $u_\rho - z(2b_\alpha^\lambda u_\lambda + u_{3,\alpha})$.

As a consequences mathematical studies of thick shells are based models that need to be improved. Here, a 2D shell kinematic equations that introduce a particular form of admissible displacements obtained as a solution of a torsional loading problem in 3D solid is used here to derive a new exact laminated shell model

*Corresponding author
Email address: arnongatcha@gmail.com (Arno Roland Ngatcha Ndengna)

for the study of the mechanical behavior of laminated shells. In this framework the magnitude of transverse displacement (stretching displacement) does not compared to shell thickness.

For the multilayered shell analysis, the literature offers several 3D exact model coupling the in-plane and out-of-plane strains and derived from 3D field displacement. These models are often solved analytically (by a simple algorithm, Navier or Ritz-Raleigh approaches) as in [21], [22] or numerically by FEM (Finite Element Method) as in [27],[35]. The models widely used in literature neglect the section warping plane, the stretching-through-thickness and the Gauss tensor effects. The model available in literature are not able to reproduce the mechanical behavior of 3D shell under twist load accurately. Moreover, several 3D exact model have been developed for a particular geometry, sequence of layers, choice of materials, type of loadings. We develop and implement a 3D exact model for multilayered shell (seen as a 2D exact model which account the transverse strains) having a very large field of application and not use any and-hoc assumption and correction factor as in Reissner-Minddlin (R-M) based models or more generally the model based on First-order Shear Deformation Theories (FSDT). The proposed theory does not admits any limitation on the type of loading applied to the laminated shell. The developed 3D laminate constitutive equations (LCE) serve to derive a exact model capable to address the variations in the thickness.

Classical or more recent Shell models for multilayered composite double curvature shells result in a system of several coupled second order differential equations in term of displacement fields u ,v, w. The classical laminated shell theory (CLST) results in a system containing three sub-matrices A, B, D more used in literature (and initially developed for plates by [32]). In the same way, the First-order Shear Deformation (FSD) based models also widely used in literature, provides a system constituted of fourth sub-matrices A, B, D(in plane stresses) and F depending of correction factor in the transverse plane. The above sub-matrices are often derived from Hooke's laws (assuming the stress plane) without geometry parameters and the curvature of the shell. This law reads [4] [27],[32]:

$$\sigma^{\alpha\beta} = [\overline{Q}]\epsilon^{\alpha\beta}, \tag{1}$$

where $\alpha, \beta = 1, 2$ are the problem physical coordinates, $[\overline{Q}] = \overline{Q}_{mn}, \quad m, n = 1, 2, 6$ is the reduced material matrix. The above sub-matrices were widely used in the literature to analyze the mechanical behavior of LCS (see for instance [1], [2], [3], [4], [5], [8],[9], [27],[31],[36]). When we assume the stress plane, $\sigma^{\alpha 3} = 0$ and $\sigma^{33} = 0$ and in this case, some terms appear in the constitutive relation. These terms is practically ignored in some formulations of mechanical behavior of LCS available in the literature and widely used by several authors. Really the Hooke's law at the first order for two-dimensional laminated composite shells using the same assumption and geometric parameters reads[23]:

$$\sigma^{\alpha\beta} = L^{\alpha\beta\rho\gamma}(\mathbf{x}, 0)\epsilon_{\gamma\rho}, \tag{2}$$

where

$$L^{\alpha\beta\rho\gamma}(\mathbf{x}, 0) = C^{\alpha\beta\gamma\delta} - 2C^{\alpha\beta\gamma\delta}\left[(2C^{\gamma 3\alpha 3})^{-1}C^{\rho 3\gamma\delta}(2C^{\gamma 333})^{-1}\right] - C^{\alpha\beta 33}\left[(2C^{\gamma 333})^{-1}C^{\rho 3\gamma\delta} + C^{3333})^{-1}C^{33\gamma\delta}\right], \tag{3}$$

where $C^{\alpha\beta\rho\gamma}$ is the matrix of material. For certain application, we get we can take:

$$L^{\alpha\beta\rho\gamma}(\mathbf{x}, 0) = a^{\alpha\beta}a^{\gamma\rho}\left([Q] - \frac{I}{Q_{66}}\right), \tag{4}$$

where $a^{\alpha\beta}$ is the first fundamental form of the shell. When the thickness of the laminated shell becomes greater, the CLST is not applicable as proved in Ngatcha et al.,[21] and extensional-twisting-shear, extensional-Gauss bending-shearing, Gauss bending-shearing are of mechanical couplings which can not found via a correction factor (used for isotropic materials) without physical and mechanical justifications as in FSD based models. In such case, the shell models for multilayered composite double curvature shells can resulted from a system including five sub-matrices A, B, C D and E (ABCDE-matrix) [21, 22]:

$$\mathbf{N} = \bar{A}e - \bar{B}K + \bar{C}Q; \quad \mathbf{M} = -\bar{B}e + \bar{C}K - \bar{D}Q; \quad \mathbf{M}^* = \bar{C}e - \bar{D}K + \bar{E}Q; \tag{5}$$

where

$$\begin{aligned}\bar{A} &= \bar{A}_{ij} = A_{ij} + K_\alpha B_{ij},\ \bar{B} = \bar{B}_{ij} = B_{ij} + K_\alpha C_{ij},\\ \bar{C} &= \bar{C}_{ij} = C_{ij} + K_\alpha D_{ij}, \bar{D} = \bar{D}_{ij} = D_{ij} + K_\alpha E_{ij},\\ \bar{E} &= \bar{E}_{ij} = E_{ij} + K_\alpha T_{ij},\end{aligned} \tag{6}$$

and where $K_\alpha = \frac{C}{R_\alpha}$ with C the tracer and R_α the radii of composite shells. The force and moments are $\mathbf{N}, \mathbf{M}, \mathbf{M}^*$ and the deformation tensors are e, K and Q (see below). We observe that the ABCDE-matrix is more interesting than ABD-matrix of CLST or ABDF-matrix of FSDT. In high order shell theories which include transverse normal strains, the high order terms are introduced only in kinematic equations. It's important to know that the variations in the thickness can produces the warping sections effect during the deformation. A warping tensor $\overline{q}\Upsilon_{\alpha\beta}$ must appear in plane deformation tensor. Here, the term $\overline{q}$ is defined such that the stretching-through-the-thickness term q is given by $q(x, y, z) = \sum_i z^i \overline{q}(x, y)$. The effects of thickness stretching in analysis of LCS have been investigated by [8]. Therefore the Warping and its effects due to "stretching-through-the-thickness" variable must be considered for any analysis of three-dimensional laminated composite and sandwich structures.

In view to integrate the geometric and curvature parameters of 3D shells, the following equation is the most general(anisotropic) possible for each lamina has been used to find a generalized ABCDE-matrix (from 3D constitutive relation) proposed to the first time in this work:

$$\sigma^{ij} = L^{ijkl}\epsilon_{kl}, \tag{7}$$

where $i, j = x, y, z$ are the problem physical coordinates and where $L^{ijkl} = [\overline{Q}]G^{ij}G^{kl}$ is the matrix satisfying the ellipticity condition. i.e. there exist a constant $a > 0$ such that for any symmetric tensor χ we have $L^{ijkl}\chi_{ij}\chi_{kl} \geq a\chi_{kl}\chi_{kl}$. The tensor G^{ij} is the first fundamental form for 3D shell that accounts the geometric and curvature parameters of the shell.

For exact analysis of laminated plates and shell several method can be used: closed form solution, space-state based formulation, Fourier series expansion, approximation of the in-plane displacement through the thickness, direct elasticity based approach. All these approaches or theories can be found in several papers in the literature. Closed form solution can be considered only for cross-ply laminated (which means that the fibre orientation angle equals 0^o or 90^o). The use of elasticity based approach directly, can neglect some mechanical couplings appearing in the LCE. Moreover, the mechanical behavior at macro-level of the composite structure cannot be well formulated and can lead to erroneous results. The series expansion method may contains terms that are difficult to manipulate. A exact analysis of laminated shells accounting more possible mechanical couplings cited above and describing a complete mechanical behavior at macro-level is still necessary and to be welcome. The literature offers many 3D models for one-layered and multilayered isotropic, orthotropic, sandwich and composite plate structures. Really,such models or theories are not applicable for static and dynamic analysis laminated shells. Exact three-dimensional models for one-layered and multilayered isotropic, orthotropic, sandwich and composite structures were developed for static and free vibration analysis of plates and shells in terms of displacements with in-plane and out-of-plane stresses through the thickness direction [5], [8]. In the work of Carrera et al.,[8], the 3D exact solution is based on the differential equations of equilibrium written in general orthogonal curvilinear coordinates. This exact method is based on a layer-wise approach, the continuity of displacements and transverse shear/normal stresses is imposed at the interfaces between the layers of the structure. A model to analyze the LCS has been developed using same approach and coupled with the principle of energy minimization by [16]. Using directly elasticity equations, exact solution using the potential of 3D spherical equations for composite structures in open and finite domains were obtained by [29**?**](see also [30]). The results of Ren [29] were compared with classical and Donell's shell theory. Based on exact elasticity theory, a 3D exact model is derived for analysis of free vibration of cylindrical shells has been developed by Gasemzadeh et al., [11]. A such method is also used by [33] to find exact solution (displacement and stress fields) for analysis of cylindrical shell panels via a displacement-based formulation obtained directly by a elasticity problem. Tornabene et al., [35] have developed a dynamic formulation(exact models) for free vibration analysis of cylindrical and spherical shell panels. In Reddy [27], exact 2D/3D

models and solutions are developed on the basis of three-dimensional elasticity theory, layer-wise approach and equivalent-layer approach for the static and dynamic analysis of LCS. Ngatcha et al.,[22] have recently presented and implemented a more general two-dimensional exact model for transient and static analysis of thin and moderately thick shell without the effect of stretching-through-the-thickness term in kinematic equations and neglecting the warping sections. An approach to find by simple calculation the strains/stress in each layer has been proposed by Ngatcha et al., [21]. The approach was more appropriate to analyze the tube composite structure without any difficulty. The formulations using ABCDE-matrix proposed by Ngatcha et al., [20, 21] extend some results of [27] and [4] and improve many 2D laminated shell theories recently developed and used to design composite shell structures.

Several above 3D static investigations neglect the effect of warping tensor that produce some mechanical couplings in the material during the deformation. For dynamic analysis using above models, only the term $I_0\ddot{w}$ is considered. Some terms related to $\ddot{w}$ as the Morozov term and the term $\left(I_2 A^{\alpha}\tau + I_4 A^{\alpha\tau} b_{\nu}^{\gamma} b_{\gamma}^{\nu}\right) \nabla_{\alpha}\nabla_{\tau}\ddot{w}$, where $I_i, i = 0, 2, 4$ is the inertial term (see below) do not appear. Moreover, the constitutive relations used in some above models are not genuinely 3D and some plane and transverse mechanical couplings do not appear.

We develop in the current study a novel 3D laminated constitutive equations that contains capitals information to analyze a composite shell or plate structure. It's expected that this 3D LCE is one of most general encountered in the literature due to the presence of novel elements in the stiffness matrix embodying mechanically coupled deformation such as extensional-bending-shearing, bending-shearing, extensional-twisting-shearing, extensional-bending-shearing, extensional-twisting, extensional-stretching bending-stretching, shearing-stretching and stretching couplings. Such matrix provides critical and capitals information on the mechanical behavior of shell structure at the macro-level. All these information are used to improve the 3D exact solutions obtained by other methods. Some shell models are not physically and mathematically justified. It's necessary to use a rigorous laminate constitutive equations to develop accurate modelings to investigate by analytical method center deflection, natural frequencies, membrane displacement, local stress and strains of the composite laminated shells. The developed LCE contain the LCE obtained by CLST and by FSDT with additional terms related to the third fundamental form, warping section tensor and the thickness variation during the deformation that governing strain energy.

The first objective of this paper is to derive a novel 3D laminated constitutive relations that contains several mechanical couplings necessary to design efficiency composite shell structures. The second objective is to use this constitutive relation to derive using Hamilton's principle a new 3D exact model for the dynamic and static analysis of the behavior of laminated composite plates and shells. The obtained 3D exact model no use any and-hoc assumption and correction factor as in several recent works available in literature dealing the composite materials. The third objective is to extended this exact model to doubly curved laminated composite shells to find a original 3D matrix. To the best of authors knowledge, there is no published works in the literature developing non heuristic 3D exact model for the static and dynamic behavior of laminated composite doubly curved shells. That not only includes the warping and the twisting effects but also accounts the thickness variation during the deformation of the laminated using a stretching-through-the-thickness term. I performed in this work the static and natural vibration analysis of cross-ply laminate composite doubly curved shell to determine Navier's solution with the simply supported boundary condition at all edges. The goal of this paper is to derive and implement analytically a new 3D exact model to 3D accurate analyze of the static and transient behavior of a LCS. The rest of paper is presented as follows. The section 2, we present a three-dimensional laminated shell model and some assumptions used in this modeling. We proof the existence of a admissible displacement by a natural way. We propose also a existence and uniqueness theorem for the shell model. In section **??**, we develop a new 3D constitutive equations using the Hooke's law with geometric and curvature effects. We propose using Hamilton's principle and the proposed 3D LCE a new exact model. Here Navier based method is used to obtain a general dynamic 3D equations to solve a 3D torsion problem with accuracy in section 4. We perform some tests and Benchmarks to validate the proposed 3D LCE and the exact models in section 5. The exact analysis proposed in this work can be extended to other mechanical contexts in composite materials.

2 A three-dimensional laminated shell model

In this section, we extend a 2D shell formulation of [**?**] also derived from a 3D linear elastic isotropic material (by introducing a particular from of admissible displacement obtained as a solution of a torsional loading problem in 3D solid) to linear anisotropic shell formulation. Here, transversal shear strains and thickness variation are accountable through additional terms which appear in the final kinematic equations. In the case of thick shell it is possible observed that the effect of shear deformation with a weak core and facing as well as laminated composite shells with large ratios of the tangential elastic modulus(E_2) to the transverse shear modulus (G_{12}) is important[1].

Assumptions

Let assume in addition for a current modeling purpose that:
(i) Each constituent layer has its own geometrical and physico-mechanical characteristics; (ii) the material of each constituent layer is linearly elastic and anisotropic; (iii) the layers are in perfect bond, no slip between two adjacent laminae may occur;(iv) the displacement field function in the thickness direction is assumed to be constant or linearly varying the throughout the thickness; (v) the mid-surface of the laminated and the each laminae is bounded and sufficiently smooth for all subsequent computations. (vi) The perfect-bonding conditions for the layers are formulated as follows: the stresses $\sigma(x,y,z)$ and displacements $U_i(x,y,z)$ are continuous at the interface between the $(k-1)th$ and kth layers:

$$\begin{cases} U_i^k|_{\Gamma_{k-1,k}} = U_i^{k-1}|_{\Gamma_{k-1,k}}, \\ [\sigma]_k \mathbf{n}_{i,k} = -[\sigma]_k \mathbf{n}_{i,k-1}. \end{cases} \tag{8}$$

where $\Gamma_{k-1,k}$ (see Fig. **??** on page **??**) is the interface between the layer $k-1$ and k; $\mathbf{n}_{i,k}$(respectively $\mathbf{n}_{i,k-1}$) is the normal of layer k(respectively of layer $k-1$) along the direction i.
We note that $\mathbf{n}_i$ is the components of the normal $\widehat{n}$ to the interface along the direction i where $\widehat{n}$ is the normal of domain Ω_k given by

$$\widehat{n} = (n_\alpha, n_\beta) = (\cos(\varphi_\alpha), \cos(\varphi_\beta)) \tag{9}$$

where φ_α and φ_β are the angles between the normal $\widehat{n}$ and the directions α and β, respectively.

2.1 Existence of a potential distortion and kinematic equations

Mid-surface displacement $\widetilde{u}(x,y,z)$ is computed in order to satisfy the plane strain state and the change of surface along the thickness $U_\alpha(x,y,z) = \mu_\alpha^\lambda \widetilde{u}_\lambda$ where $\mu_\gamma^\rho = \delta_\gamma^\rho - z b_\gamma^\rho$. In this case $2\epsilon_{\alpha 3} = 0$ and u_3 does not depend on z-parameter. The general solution of Equation $2\epsilon_{\alpha 3} = 0$ is found in Nzengwa et al [25] and consists to find $\widetilde{u}_\alpha$ in the base (a_α, a_3) that satisfies Equations (10)

$$\begin{cases} \widetilde{u}_\gamma(x,y,z) = \mu_\gamma^\rho u_\rho(\alpha,\beta) - z u_{3,\gamma}; & \text{for each}(u_\rho, u_3) \in (T_{\mathbf{x}}S)^2 \\ \widetilde{u}_3(\alpha,\beta,z) = u_3(\alpha,\beta) \end{cases} \tag{10}$$

We note that the transverse strains is given by

$$\epsilon_{\alpha 3} = \frac{1}{2}(\mu_\alpha^\rho \widetilde{u}_{\rho,3} + (\widetilde{u}_{\rho,3} + B_\alpha^\rho \widetilde{u}_\rho))$$

Let us $\phi = (\phi_\alpha, \phi_3)$ the total field of transverse deformation where $\phi_\alpha = 2\epsilon_{\alpha 3} \quad \alpha = 1,2$ and where $\phi_3 = \epsilon_{33}$.

[1] We can have in this situation $G_{12} = \lambda E_2$ with $\lambda \geq 0.5$

Proof of existence of a admissible displacement $q(x, y, z)$

Admitting that $rot(\phi) = 0$, there exist a function $q(x, y, z)$ whose derive ϕ and in this case, we have:

$$\phi_\alpha = \nabla_\alpha q = 2\epsilon_{\alpha 3}, \quad \text{and} \quad \phi_3 = \partial_3 q = \epsilon_{33}. \tag{11}$$

We recall that

$$\begin{cases} U_\alpha(x, y, z) = (\mu)^\beta_\alpha u_\alpha(\mathbf{x}) - z u_{3,\alpha}(\mathbf{x}), & \text{in} \quad \Omega, \\ U_3(\mathbf{x}, z) = u_3(\mathbf{x}), \end{cases} \tag{12}$$

We multiply the first equation of (47) by $(\mu^{-1})^\beta_\alpha$ and we obtain:

$$(\mu^{-1})^\alpha_\beta U_\alpha(x, y, z) = u_\beta(\mathbf{x}) - z(\mu^{-1})^\alpha_\beta \widetilde{u}_{3,\alpha}(\mathbf{x}). \tag{13}$$

We derive with respect to z and we get:

$$\left((\mu^{-1})^\alpha_\beta U_\alpha(x, y, z)\right) = -\left(z(\mu^{-1})^\alpha_\beta U_{\alpha,3}(\mathbf{x})\right) = -(\mu^{-1})^\rho_\beta(\mu^{-1})^\alpha_\rho(\widetilde{u}_3)_{,z} + (\mu^{-1})^\rho_\beta(\mu^{-1})^\alpha_\rho q_{,\alpha}, \tag{14}$$

since we have:

$$(z(\mu^{-1})^\alpha_\beta \widetilde{u}_{3,\alpha})_{,z} = (\mu^{-1})^\rho_\beta(\mu^{-1})^\alpha_\rho \widetilde{u}_{3,\alpha} - (\mu^{-1})^\rho_\beta(\mu^{-1})^\alpha_\rho(\widetilde{u}_{3,z})_{,\alpha}. \tag{15}$$

Due to fact that $\widetilde{u}_3 = \partial_3 q = \partial_z q$, we have $(\widetilde{u}_{3,z})_{,\alpha} = q_{,\alpha}$. Therefore, $q(x, y, z)$ satisfies the following additional system of equations:

$$\begin{cases} \left((\mu^{-1})^\rho_\alpha \widetilde{u}_\alpha(x, y, z)\right)_{,z} + (\mu^{-1})^\rho_\beta(\mu^{-1})^\alpha_\rho \partial_\alpha\left(\widetilde{u}_3 - q\right) = 0 \\ (\widetilde{u}_3)_{,z} = q_{,z} \end{cases} \tag{16}$$

The last equation of (16) implies the existence of normal displacement depending only of $\mathbf{x}$. Noting u_3 this displacement, we get:

$$((\widetilde{u}_3) - q)_{,z} = 0 \Rightarrow u_3(x, y) = \widetilde{u}_3 - q. \tag{17}$$

With (16) and (17) we have proven the existence of admissible displacement q (stretching function) by using a 3D torsion problem. It's possible to write a 2D kinematic with through-the-thickness variable.

A 2D kinematic with through-the-thickness variable: 3D Kinematic equations

The stretching function introduce the transverse displacement and the kinematic thick shell equations developed in [26] and reformulated as follows:

$$\begin{cases} U_1(\mathbf{x}, z) = (1 - z/R_1)u_1(\mathbf{x}) - z\theta_1(\mathbf{x}) + z^2\Phi_1(\mathbf{x}), & \text{in} \quad \Omega, \\ U_2(\mathbf{x}, z) = (1 - z/R_2)u_2(\mathbf{x}) - z\theta_2(\mathbf{x}) + z^2\Phi_2(\mathbf{x}), & \text{in} \quad \Omega \\ U_3(\mathbf{x}, z) = u_3(\mathbf{x}) + q(\mathbf{x}, z). & \text{in} \quad \Omega \end{cases} \tag{18}$$

Here, θ_α are the rotations of the normal of the mid-surface, given in curvilinear coordinates by $\theta_\alpha = \theta_\rho(u_\alpha) = (u_{3,\alpha} + B^\rho_\alpha u_\rho)$. The vector Φ_α are the Gauss rotations of the mid-surface: $\Phi_\alpha = (B^\rho_\gamma B^\gamma_\alpha u_\rho + B^\rho_\alpha u_{3,\rho})$. The function $q(\mathbf{x}, z))$ is the stretching displacement through the thickness. The reformulated shell model contains the classical Kirchhoff-Love(K-L) displacement $u_\rho - z(2b^\lambda_\alpha u_\lambda + u_{3,\alpha})$ or that found in Reissner-Mindlin(R-M) model $u_\rho - z(2b^\lambda_\rho u_\lambda + \varpi_\rho)$. The third term which is partly proportional to $\chi = \dfrac{h}{2R}$ (thickness ratio) and χ^2 vanish in K-L and R-M shell models.

Explanation of the term $q(\mathbf{x}, z)$

The term $q(\mathbf{x}, z)$ is a particular admissible displacement and can be expressed as a function (non polynomial or polynomial) in z:

$$q(\mathbf{x}, z) = w(z)\overline{q}(\mathbf{x}). \tag{19}$$

where $w(z)$ is the transverse distribution function. The term $q(\mathbf{x}, z)$ is the **stretching-through-the-thickness** and provides the transverse normal deformation/stress contributions in the laminated composite shells. More generally, we have:

$$q(x, z) = \overline{q}(\mathbf{x}, 0) + z\overline{q}_1(\mathbf{x}) + z^2\overline{q}_2(\mathbf{x}) + ... + z^n\overline{q}_n(\mathbf{x}). \tag{20}$$

When $z = 0$, we find $q(\mathbf{x}, z) = 0$ and we retrieve the model proposed in [25]. the K-L based kinematic or FSD based models. The order of this term determine the refinement of 3D exact solutions of the composite shell problems. In first order, we read

$$q(\mathbf{x}, z) = z\overline{q}(\mathbf{x}) = w(z)\overline{q}(\mathbf{x}) \quad \text{where} \quad w(z) = z. \tag{21}$$

In this paper we have taken $q(\mathbf{x}, z)$ at the first order.

2.2 Strain-Displacement field using equivalent layer approach with through-the-thickness variable kinematic

The stress-strain relationship for a typical $k-th$ lamina in a laminated composite shell made of N laminas $1 \leq k \leq N$ (see Fig.(1)) is written in local basis by Hooke equation:

$$\sigma_{ij}^k = [\overline{Q}(\theta_k)]\epsilon_{ij}^k \tag{22}$$

where σ_{ij}^k, ϵ_{ij}^k, $[\overline{Q}(\theta_k)]$ represent the 3D stress tensor, 3D strain tensor, and 3D reduced stiffness matrix, respectively.

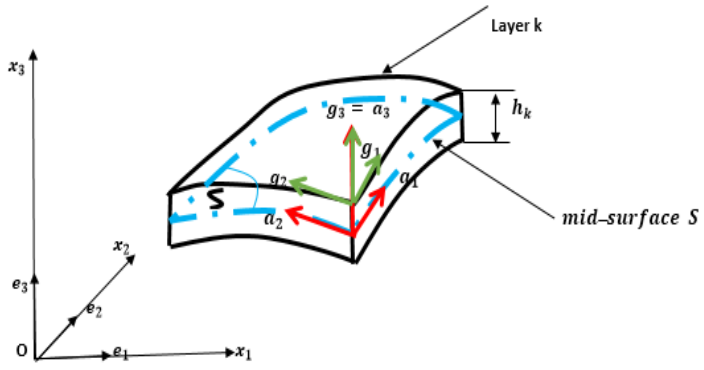

Figure 1: One layer of laminate shell.

Let $\widetilde{U}(\eta,q)=(U(\eta),U(q))$ where $U(\eta)=(U_\alpha(\eta),U_3(\eta))$, $U(q)=(0,0,q)$. The 3D strain tensor components are given as:

$$\epsilon^k(\widetilde{U})=\begin{cases}\epsilon^k_{\alpha\beta}(U)=e^k_{\alpha\beta}(\widetilde{u})-z^kK^k_{\alpha\beta}(\widetilde{u})+(z^2)^kQ^k_{\alpha\beta}(\widetilde{u})+q^k\Upsilon^k_{\alpha\beta}\\ \epsilon^k_{\alpha3}(U)=\dfrac{1}{2}(\mu^\rho_\alpha\widetilde{u}^k_{\rho,3}+(\widetilde{u}^k_{\rho,3}+B^\rho_\alpha\widetilde{u}^k_\rho))\\ \epsilon^k_{33}(U)=U^k_{3,3}\end{cases}\tag{23}$$

$$\overline{\epsilon}^k(\widetilde{U})=\begin{cases}\epsilon^k_{\alpha\beta}(U)=e^k_{\alpha\beta}(\widetilde{u})-z^kK^k_{\alpha\beta}(\widetilde{u})+(z^2)^kQ^k_{\alpha\beta}(\widetilde{u})\\ \epsilon^k_{i3}(U(\eta))=0=\epsilon^\eta_{i3}\\ \epsilon^k_{\alpha\beta}(U(q))=q^k(\mathbf{x},z)\Upsilon^k_{\alpha\beta}(\mathbf{x},z)=\epsilon^q\\ \epsilon^k_{\alpha3}(U(q))=\dfrac{1}{2}\partial_\alpha q^k(\mathbf{x},z)=\dfrac{1}{2}\phi^k_\alpha\\ \epsilon_{33}(q)=\partial_3q^k=\phi^k_3\end{cases}\tag{24}$$

where $\gamma_{\alpha\beta}=-(\mu^\nu_\alpha b_{\nu\beta}+\mu^\nu_\beta b_{\nu\alpha})$, and $q(\mathbf{x},z)=w(z)\overline{q}(\mathbf{x})$. Finally, the 3D strain tensor which accounts is given by:

$$\epsilon_{ij}(\widetilde{U})=\epsilon_{ij}(U(\eta))+\epsilon_{ij}(U(q))=\epsilon^\eta+\epsilon^q,\tag{25}$$

where we have $\widetilde{U}=\widetilde{U}(U)+\widetilde{U}(q)$.

For orthotropic material the stress-strain constitutive relations is given by Equation (26):

$$\overline{\sigma}^k=\begin{cases}\left[\sigma^k_{\alpha\beta}\right]=[\overline{Q}][e_{\alpha\beta}]-z[\overline{Q}][K_{\alpha\beta}]+(z^2)^k[\overline{Q}][Q^k_{\alpha\beta}]+q^k[\overline{Q}][\Upsilon^k_{\alpha\beta}],\\ [\sigma^k_{\alpha3}]=\dfrac{1}{2}[\overline{Q}][\phi^k_\alpha],\\ [\sigma^k_{33}]=[\overline{Q}][\phi^k_3],\end{cases}\tag{26}$$

and for each layer, the micro-mechanical behavior is given by (27)

$$\begin{aligned}[\bar{\sigma}]_k &= [\overline{Q}(\theta_k)][e_{\alpha\beta}]^k-z_k[\overline{Q}(\theta_k)][K_{\alpha\beta}]^k+z_k^2[\overline{Q}(\theta_k)][Q_{\alpha\beta}]^k+[\overline{Q}(\theta_k)][q\Upsilon_{\alpha\beta}]^k\\ &+ 1/2[\overline{Q}(\theta_k)][\phi_\alpha]^k+[\overline{Q}(\theta_k)][\phi_3]^k,\end{aligned}\tag{27}$$

where $\mathbf{e}_{\alpha\beta}(\widetilde{u})$, $\mathbf{K}_{\alpha\beta}(\widetilde{u})$, $\mathbf{Q}_{\alpha\beta}(\widetilde{u})$ and $q\Upsilon_{\alpha\beta}$ define respectively, the membrane deformation tensor, the change of curvature tensor, the change in third fundamental form (or gauss curvature tensor) and the warping in-plane tensor. We have:

$$\begin{aligned}\mathbf{e}_{\alpha\beta}(\widetilde{u}) &= \frac{1}{2}(\nabla_\beta u_\alpha+\nabla_\alpha u_\beta-2u_3b_{\alpha\beta});\\ \mathbf{K}_{\alpha\beta}(\widetilde{u}) &= \nabla_\alpha b^\rho_\beta u_\rho+b^\rho_\alpha\nabla_\beta u_\rho+b^\rho_\beta\nabla_\alpha u_\rho+\nabla_\alpha\nabla_\beta u_3-b^\tau_\alpha b_{\tau\beta}u_3;\\ 2\mathbf{Q}_{\alpha\beta}(\widetilde{u}) &= b^\rho_\alpha\nabla_\beta b^\tau_\rho u_\tau+b^\rho_\alpha b^\tau_\rho\nabla_\beta u_\tau+b^\rho_\alpha\nabla_\beta\nabla_\rho u_3+b^\rho_\beta\nabla_\alpha b^\tau_\alpha u_\tau+b^\rho_\beta b^\tau_\rho\nabla_\alpha u_\tau+b^\rho_\beta\nabla_\alpha\nabla_\rho u_3;\\ \Upsilon_{\alpha\beta}q &= -\frac{1}{2}\left(\mu^\tau_\alpha b_{\tau\beta}+\mu^\tau_\beta b_{\tau\alpha}\right)q\end{aligned}\tag{28}$$

The terms $Q_{\alpha\beta}(\widetilde{u})$ (that is the product of the curvature tensor and the variation of the rotational vector) and $\Upsilon_{\alpha\beta}(\mathbf{x},z)$ disappear usually in some 2D/3D exact laminated shell models recently developed in the literature. Moreover, its effect does not include the constitutive relation used to analyze shell laminated. We remark that these tensors, referred respectively to hereafter as the Gauss deformation tensor and the warping section tensor due variation in the thickness. In curvilinear coordinates, the tensors given in Eq. (28) written as

follows[20]:

$$
\begin{aligned}
e_{\alpha\alpha} &= \frac{u_{\alpha,\alpha}}{A_\alpha} + \frac{A_{\alpha,\beta}}{A_\alpha A_\beta} u_\beta + \frac{u_3}{R_\alpha}, && (29)\\
2e_{\alpha\beta} &= \frac{u_{\alpha,\beta}}{A_\beta} - \frac{A_{\alpha,\beta}}{A_\alpha A_\beta} u_\alpha + \frac{u_{\beta,\alpha}}{A_\alpha} + \frac{A_{\beta,\alpha}}{A_\alpha A_\beta} u_\beta, && (30)\\
K_{\alpha\alpha} &= \frac{R_{\alpha,\alpha}}{A_\alpha R_\alpha^2} u_\alpha - \frac{2}{R_\alpha}\left(\frac{u_{\alpha,\alpha}}{A_\beta}\right) - \frac{A_{\alpha,\beta}}{A_\alpha A_\beta}\left(\frac{u_\beta}{R_\alpha}\right) + \frac{1}{A_\alpha}\left(\frac{u_{3,\alpha}}{A_\alpha}\right)_{,\alpha} + \frac{A_{\alpha,\beta}}{A_\alpha A_\beta}\left(\frac{u_{3,\beta}}{A_\beta}\right) - \frac{u_3}{R_\alpha^2},\\
2K_{\alpha\beta} &= \frac{R_{\alpha,\beta}}{A_\beta R_\alpha^2} u_\alpha - \frac{2}{R_\alpha}\left(\frac{u_{\alpha,\beta}}{A_\beta}\right) + \left(\frac{1}{R_\beta} + \frac{1}{R_\alpha}\right)\frac{A_{\alpha,\beta}}{A_\alpha A_\beta} u_\alpha + \frac{1}{A_\beta}\left(\frac{u_{3,\alpha}}{A_\alpha}\right)_{,\beta} - \frac{A_{\alpha,\beta}}{A_\alpha A_\beta}\left(\frac{u_{3,\alpha}}{A_\alpha}\right)\\
&+ \frac{R_{\beta,\alpha}}{A_\alpha R_\beta^2} u_\beta - \frac{2}{R_\beta}\left(\frac{u_{\beta,\alpha}}{A_\alpha}\right) + \left(\frac{1}{R_\beta} + \frac{1}{R_\alpha}\right)\frac{A_{\beta,\alpha}}{A_\alpha A_\beta} u_\beta + \frac{1}{A_\alpha}\left(\frac{u_{3,\beta}}{A_\beta}\right)_{,\alpha} - \frac{A_{\beta,\alpha}}{A_\alpha A_\beta}\left(\frac{u_{3,\beta}}{A_\beta}\right),\\
Q_{\alpha\alpha} &= \frac{1}{R_\alpha}\left[-\frac{1}{A_\alpha}\left(\frac{u_\alpha}{R_\alpha}\right)_{,\alpha} - \frac{A_{\beta,\alpha}}{A_\alpha A_\beta}\left(\frac{u_\beta}{R_\beta}\right) + \frac{1}{A_\alpha}\left(\frac{u_{3,\alpha}}{A_\alpha}\right)_{,\alpha} + \frac{A_{\beta,\alpha}}{A_\alpha A_\beta}\left(\frac{u_{3,\beta}}{A_\beta}\right)\right],\\
2Q_{\alpha\beta} &= -\frac{1}{R_\alpha}\left[\frac{1}{A_\beta}\left(\frac{u_\alpha}{R_\alpha}\right)_{,\alpha} - \frac{A_{\beta,\alpha}}{A_\alpha A_\beta}\left(\frac{u_\alpha}{R_\beta}\right)\right] - \frac{1}{R_\beta}\left[\frac{1}{A_\alpha}\left(\frac{u_\beta}{R_\beta}\right)_{,\alpha} - \frac{A_{\beta,\alpha}}{A_\alpha A_\beta}\left(\frac{u_\beta}{R_\alpha}\right)\right]\\
&+ \frac{1}{A_\alpha A_\beta}\left(\frac{u_{3,\alpha}}{A_\alpha}\right)_{,\beta} + \frac{1}{A_\alpha A_\beta}\left(\frac{u_{3,\beta}}{A_\beta}\right)_{,\alpha} - \frac{A_{\beta,\alpha}}{A_\alpha A_\beta}\left(\frac{u_{3,\alpha}}{A_\alpha} R_\beta\right) - \frac{A_{\beta,\alpha}}{A_\alpha A_\beta}\left(\frac{u_{3,\beta}}{A_\beta R_\alpha}\right).
\end{aligned}
$$

Cylindrical surface with radius R: $\mathbf{R} = (R\cos\theta,\ R\sin\theta,\ x)$ the coordinates are $(x, R\theta) = (x_1, x_2)$:

$$
(\mathbf{e}_{\alpha\beta}) = \frac{1}{2}\begin{bmatrix} 2u_{,x} & v_{,x} + \frac{1}{R}u_{,\theta} \\ * & \frac{2}{R}(v_{,\theta} + w) \end{bmatrix}, \qquad (31)
$$

$$
(\mathbf{K}_{\alpha\beta}) = \begin{bmatrix} w_{,xx} & \frac{1}{R}(w_{,x\theta} - v_{,x}) \\ * & -\frac{1}{R^2}(2v_{,\theta} + w - w_{,\theta\theta}) \end{bmatrix}, \qquad (32)
$$

$$
(\mathbf{Q}_{\alpha\beta}) = \frac{1}{2}\begin{bmatrix} 0 & \frac{1}{R^2}(v_{,x} - w_{,x\theta}) \\ * & -\frac{2}{R^3}(v_{,\theta} - w_{,\theta\theta}) \end{bmatrix} \qquad (33)
$$

For spherical surface, $\mathbf{R} = R\,(\sin\psi\cos\varphi,\, \sin\psi\sin\varphi,\, cos\psi)$. The coordinates are $(\psi, \varphi) = (x_1, x_2)$:

$$(\mathbf{e}_{\alpha\beta}) = \frac{1}{2}\begin{bmatrix} 2u_{,\alpha} + 2Rw & v_{,\alpha} + u_{,\beta} - 2v\cot\psi \\ * & 2(v_{,\beta} + wR\sin^2\psi) \end{bmatrix}, \tag{34}$$

$$(\mathbf{K}_{\alpha\beta}) = \begin{bmatrix} w_{,\alpha\alpha} - w - \frac{2}{R}u_{,\alpha} & \frac{2}{R}v\cot\psi - \frac{1}{R}(v_{,\alpha} + u_{,\beta}) \\ & +w_{,\alpha\beta} - w_{,\beta}\cot\psi \\ * & -\frac{2}{R}(v_{,\beta} + u\sin\psi\cos\psi) + \\ & w_{,\beta\beta} + w_{,\alpha}\sin\psi\cos\psi - w\sin\psi^2 \end{bmatrix}, \tag{35}$$

$$(\mathbf{Q}_{\alpha\beta}) = \frac{1}{2}\begin{bmatrix} -\frac{w_{,\alpha\alpha}}{R} + \frac{u_{,\alpha}}{R^2} & \frac{1}{R^2}(u_{,\beta} - 2v\cot\psi + v_{,\alpha}) \\ & -\frac{2}{R}(w_{,\alpha\beta} - w_{,\beta}\cot\psi) \\ * & \frac{1}{R^2}(v_{,\beta} + u\sin\psi\cos\psi) \\ & -\frac{1}{R}(w_{,\beta\beta} + w_{,\alpha}sin\psi\cos\psi) \end{bmatrix} \tag{36}$$

3 Constitutive relation: 3D General composite-shell stiffness coefficients for geometrically thick shells

Each lamina is considered to be orthotropic and linearly elastic. The stress-strain relation for thick lamina (see Fig.(1)) is:

$$\begin{pmatrix} \sigma_{xx} \\ \sigma_{yy} \\ \sigma_{zz} \\ \sigma_{xz} \\ \sigma_{yz} \\ \sigma_{xy} \end{pmatrix}_k = \begin{pmatrix} \overline{Q}_{11} & \overline{Q}_{12} & \overline{Q}_{13} & 0 & 0 & \overline{Q}_{16} \\ \overline{Q}_{12} & \overline{Q}_{22} & \overline{Q}_{23} & 0 & 0 & \overline{Q}_{26} \\ \overline{Q}_{13} & \overline{Q}_{23} & \overline{Q}_{33} & 0 & 0 & \overline{Q}_{36} \\ 0 & 0 & 0 & \overline{Q}_{44} & \overline{Q}_{45} & 0 \\ 0 & 0 & 0 & \overline{Q}_{54} & \overline{Q}_{55} & 0 \\ \overline{Q}_{16} & \overline{Q}_{26} & \overline{Q}_{36} & 0 & 0 & \overline{Q}_{66} \end{pmatrix} \begin{pmatrix} \epsilon_{xx} \\ \epsilon_{yy} \\ \epsilon_{zz} \\ \epsilon_{xz} \\ \epsilon_{yz} \\ \epsilon_{xy} \end{pmatrix}_k \tag{37}$$

(x, y, z) are the problem coordinates. in curvilinear coordinates we have:

$$(\sigma^{ij})_k = [\overline{Q}(\theta_k)]g^{ij}g^{kl}(\epsilon_{kl})_k \tag{38}$$

where k denotes the $k-layer$ of the multilayered shell plotted in Fig. (2). These Equations are the relationship between the components of stress in (x, y, z) and (e_1, e_2, e_3) coordinate systems.
$\sigma_i^k = [Q]_k\epsilon_i^k$ and $\sigma_{ij}^k = [\overline{Q}]_k\epsilon_{ij}^k$ where k denotes the k-layer of the multilayered shell; σ_{ij} and ϵ_{ij} denotes respectively the components stress and components strains in the problem (P) coordinates (x, y, z); and σ_i and ϵ_i denotes respectively the components stress and components strains in the material (m) coordinates (e_1, e_2, e_3). Distributed in the plane (for $i = 1, 2, 6$) and outside of plane (for $i = 3, 4, 5$).
$[Q]$ is reduced stiffness matrix, and $[\overline{Q}]$ is the transformed reduced stiffness matrix. The elements of the $[Q]$ matrix above are dependent on the material constants and may be calculate as:

$$\begin{aligned} Q_{11} &= \frac{1-\nu_{32}\nu_{23}}{\Delta}E_{11}, \quad Q_{22} = \frac{1-\nu_{13}\nu_{31}}{\Delta}E_{22}, \quad Q_{33} = \frac{1-\nu_{12}\nu_{21}}{\Delta}E_{33}, \\ Q_{12} &= \frac{\nu_{12}-\nu_{13}\nu_{32}}{\Delta}E_{22}, \quad Q_{13} = \frac{\nu_{13}-\nu_{12}\nu_{23}}{\Delta}E_{33}, \quad Q_{13} = \frac{\nu_{23}-\nu_{21}\nu_{13}}{\Delta}E_{33}, \\ Q_{44} &= G_{23}, \quad Q_{55} = G_{31}, \quad Q_{66} = G_{12}, \end{aligned} \tag{39}$$

where $\Delta = 1 - \nu_{12}\nu_{21} - \nu_{23}\nu_{32} - \nu_{31}\nu_{13} - 2\nu_{21}\nu_{32}\nu_{13}$.

We note that $E_{1,2,3}$ are young modulus in directions 1, 2 and 3; G_{23} , G_{31}, G_{12} are the shear modulus in the 1-2, 1-3, 2-3 planes; $\nu_{12,21}$, $\nu_{13,31}$, $\nu_{23,32}$ are the poisson's ratios in the 1-2, 2-1, 1-3, 3-1, 2-3 and 3-2 planes. The matrix $[\overline{Q}]$ is given by:

$$[\overline{Q}] = [T]^{-1}[Q][R][T][R]^{-1}. \tag{40}$$

There $[T]$ is the transformation matrix ; $[R]$ is the Reuter matrix. These matrices are given by equation (41) in 3D:

$$T = \begin{pmatrix} c^2 & s^2 & 0 & 0 & 0 & 2cs \\ s^2 & c^2 & 0 & 0 & 0 & -2cs \\ 0 & 0 & 1 & 0 & 0 & 0 \\ 0 & 0 & 0 & c & -s & 0 \\ 0 & 0 & 0 & s & c & 0 \\ -cs & cs & 0 & 0 & 0 & c^2 - s^2 \end{pmatrix} \text{ and } R = \begin{pmatrix} 1 & 0 & 0 & 0 & 0 & 0 \\ 0 & 1 & 0 & 0 & 0 & 0 \\ 0 & 0 & 1 & 0 & 0 & 0 \\ 0 & 0 & 0 & 2 & 0 & 0 \\ 0 & 0 & 0 & 0 & 2 & 0 \\ 0 & 0 & 0 & 0 & 0 & 2 \end{pmatrix} \tag{41}$$

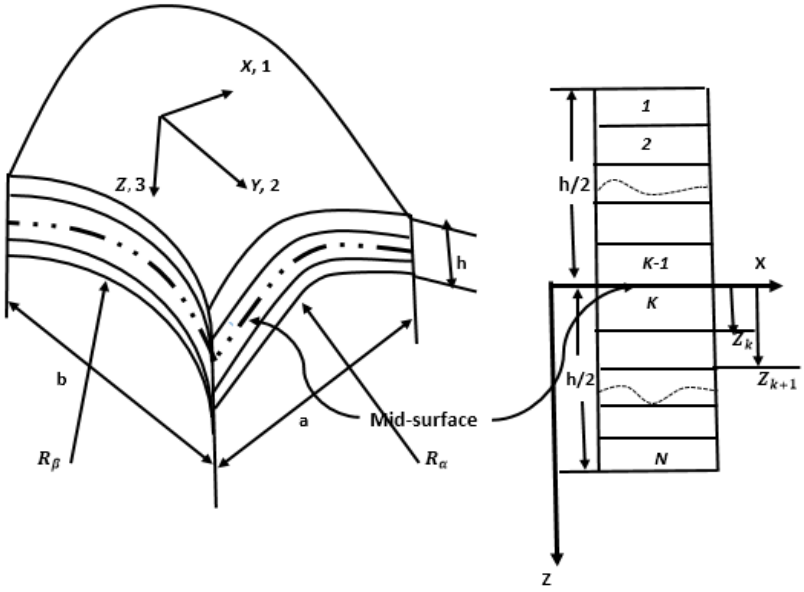

Figure 2: Description of a multilayered shell.

The novel 3D constitutive relations: Generalized ABCDE-matrix

The force and moment resultants are obtained by integrating the stresses over the shell thickness as in [22]. The stress resultant equations extend those obtained in previous work of [22] (see also [21]) and read:

$$\begin{bmatrix} N \\ M \\ M^* \\ \mathcal{S} \\ \mathcal{S}_{1z} \\ \mathcal{S}_{2z} \\ \mathcal{S}_{3z} \end{bmatrix} = \mathcal{B} = \begin{pmatrix} A & -B & C & S_1 & [0]_{6\times6} & [0]_{6\times6} & [0]_{6\times6} \\ -B & C & -D & S_2 & [0]_{6\times6} & [0]_{6\times6} & [0]_{6\times6} \\ C & -D & E & S_3 & [0]_{6\times6} & [0]_{6\times6} & [0]_{6\times6} \\ S_1 & S_2 & S_3 & S_4 & [0]_{6\times6} & [0]_{6\times6} & [0]_{6\times6} \\ [0]_{6\times6} & [0]_{6\times6} & [0]_{6\times6} & [0]_{6\times6} & S_4 & [0]_{6\times6} & [0]_{6\times6} \\ [0]_{6\times6} & [0]_{6\times6} & [0]_{6\times6} & [0]_{6\times6} & [0]_{6\times6} & S_4 & [0]_{6\times6} \\ [0]_{6\times6} & [0]_{6\times6} & [0]_{6\times6} & [0]_{6\times6} & [0]_{6\times6} & [0]_{6\times6} & S_5 \end{pmatrix} \begin{bmatrix} e \\ K \\ Q \\ \gamma\overline{q} \\ \partial_\alpha\overline{q} \\ \partial_\beta\overline{q} \\ \overline{q} \end{bmatrix} \tag{42}$$

The above equations given by (45) is the 3D laminate constitutive relations or Laminated Fundamental Law for three-dimensional thick elastic shells in first approximation. Here the effect of geometric of shell do not take into account. This methodology is also use for laminated plates in [32] and in more recent book and papers available in the literature. A such formulation is not able to give some information about the laminate tube for example. The laminate stiffness or composite-shell stiffness coefficients $A, B, C, D, ES_1, S_2, S_3, S_4, S_5$ are defined by:

$$H^l = \frac{1}{l}\sum_{k=1}^{Nb}[\overline{Q}_{ij}]_k(h_k^l - h_{k-1}^l) \quad 1 \leq i,j \leq 6, \tag{43}$$

More generally each composite-shell stiffness coefficients can be written in first approximation:

$$\mathcal{Z} = \sum_{k=1}^{Nb}[\overline{Q}_{ij}]_k \left(\int_{h_{k-1}}^{h_k} z^l w^{(t)}(z)dz\right), \quad l = 0,1,2,3,4 \quad t = 0,1,2,....,n \tag{44}$$

where the terms $[\overline{Q}_{ij}]$ are the elastic stiffness coefficients for the material. The new 3D LCE proposed in this work is different of those based on R-M type FSDT, High-order theories with through-the-thickness variable, refined theories for anisotropy shells which neglect the warping in-plane tensor. The composite-shell stiffness coefficients for 2D circular (tube for example) shells are rigorously developed in [21] and can be used for 3D laminated shell. We obtain stress and strain components from of boundary conditions and equation (**??**). We can deduce stress and strain of each layer by a complex inverse calculation and we get:

$$\begin{bmatrix} e \\ K \\ Q \\ \overline{q}\Upsilon \\ \partial_1\overline{q} \\ \partial_2\overline{q} \\ \overline{q} \end{bmatrix} = \mathcal{B} = \begin{pmatrix} A^{11} & B^{11} & C^{11} & S_1^1 & [0]_{6\times6} & [0]_{6\times6} & [0]_{6\times6} \\ E^{11} & F^{11} & G^{11} & S_2^1 & [0]_{6\times6} & [0]_{6\times6} & [0]_{6\times6} \\ I^{11} & J^{11} & K^{11} & S_3^1 & [0]_{6\times6} & [0]_{6\times6} & [0]_{6\times6} \\ S_4^1 & S_5^1 & S_6^1 & S_7^1 & [0]_{6\times6} & [0]_{6\times6} & [0]_{6\times6} \\ [0]_{6\times6} & [0]_{6\times6} & [0]_{6\times6} & [0]_{6\times6} & S_8^1 & [0]_{6\times6} & [0]_{6\times6} \\ [0]_{6\times6} & [0]_{6\times6} & [0]_{6\times6} & [0]_{6\times6} & [0]_{6\times6} & S_9^1 & [0]_{6\times6} \\ [0]_{6\times6} & [0]_{6\times6} & [0]_{6\times6} & [0]_{6\times6} & [0]_{6\times6} & [0]_{6\times6} & S_{10}^1 \end{pmatrix} \begin{bmatrix} N \\ M \\ M^* \\ \mathcal{S} \\ \mathcal{S}_{1z} \\ \mathcal{S}_{2z} \\ \mathcal{S}_{3z} \end{bmatrix} \tag{45}$$

with

$$
\begin{cases}
[A^*]=[A^{-1}],\quad [B^*]=[A^{-1}][B],\quad [C^*]=-[A^{-1}][C],\quad [D^*]=-[A^{-1}][S_1],\\
[E^*]=-[B][A^{-1}],\quad [F^*]=[A^{-1}][B]-[B][A^{-1}][B],\\
[G^*]=[B][A^{-1}][C]-[A^{-1}][C],\quad [H^*]=[B][A^{-1}][S_1]-[A^{-1}][S_1],\\
[S_1^*]=-[A^*][S_1],\quad [S_2^*]=[B][A^{-}1][S_1]+[S_2],\\
[S_3^*]=[S_3]-[C][A^{-}1][S_1],\quad [S_4^*]=[S_1][A^{-1}],\\
[S_5^*]=[S_1][A^{-1}][B]+[S_2],\quad [S_6^*]=-[S_1][A^{-1}][B]+[S_3],\\
[S_7^*]=-[S_1][A^{-1}][S_1]+[S_4],\quad [A_1^*]=[A^*]-[B^*][E^{*-1}][D^*],\\
[B_1^*]=[B^*][E^{*-1}],\quad [C_1^*]=[C^*]-[B^*][E^{*-1}][F^*],\\
[S_{11}^*]=S_1^*-[B^*][E^{*-1}][S_2^*],\quad [D_1^*]=-[E^{*-1}][D^*],\\
[E_1^*]=[E^{*-1}],\quad [F_1^*]=-[E^{*-1}][F^*],\quad [S_{21}^*]=-[E^{*-1}][S_2^*],\\
[G_1^*]=[G^*]-[H^*][E^{*-1}][D^*],\quad [H_1^*]=[H^*][E^{*-1}],\quad [I_1^*]=[I^*]-[H^*][E^{*-1}][F^*],\\
[S_{31}^*]=[S_3^*]-[H^*][E^{*-1}][S_2^*],\\
[S_{41}^*]=[S_4^*]-[S_5^*][E^{*-1}][D^*]+[S_5^*][E^{*-1}][F^*][I_1^{*-1}][G_1^*]-[S_6^*][I_1^{*-1}][G_1^*],\\
[S_{51}^*]=[S_5^*][E^{*-1}]+[S_5^*][E^{*-1}][F^*][I_1^{*-1}][H_1^*]-[S_6^*][I_1^{*-1}][H_1^*],\\
[S_{61}^*]=-[S_5^*][E^{*-1}][F^*][I_1^{*-1}]+[S_6^*][I_1^{*-1}],\\
[S_{71}^*]=-[S_5^*][E^{*-1}][S_2^*]+-[S_5^*][E^{*-1}][F^*][I_1^{*-1}][S_{31}^*]-[S_6^*][I_1^{*-1}][S_{31}^*]+[S_7^*],\\
[S_7^1]=[S_{71}^{*-1}],\quad [S_6^1]=-[S_{71}^{*-1}][S_{61}^*],\quad [S_5^1]=-[S_{71}^{*-1}][S_{51}^*],\quad [S_4^1]=-[S_{71}^{*-1}][S_{41}^*],\\
[G^{11}]=-[I_1^{*-1}][G_1^*]-[I_1^{*-1}][S_{31}^*][S_4^1],\quad [H^{11}]=-[I_1^{*-1}][H_1^*]-[I_1^{*-1}][S_{31}^*][S_5^1],\\
[I^{11}]=-[I_1^{*-1}][H_1^*]-[I_1^{*-1}][S_{31}^*][S_6^1],\quad [S_3^1]=[I_1^{*-1}][S_{31}^*][S_7^1],\\
[D^{11}]=[D_1^*]+[F_1^*][G^1]+[S_{31}^*][S_4^1],\quad [E^{11}]=[E_1^*]+[F_1^*][H^1]+[S_{21}^*][S_5^1],\\
[F^{11}]=[F_1^*][I^1]+[S_{21}^*][S_6^1],\quad [S_2^1]=[F_1^*][S_3^1]+[S_{21}^*][S_7^1],\\
[A^{11}]=[A_1^*]+[C_1^*][G^1]+[S_{11}^*][S_4^1],\quad [B^{11}]=[B_1^*]+[C_1^*][H^1]+[S_{11}^*][S_4^1],\\
[C^{11}]=[C_1^*][I^1]+[S_{11}^*][S_6^1],\quad [S_1^1]=[C_1^*][S_3^1]+[S_{11}^*][S_7^1],\\
[S_8^1]=[S_4^{-1}],\quad [S_9^1]=[S_4^{-1}],\quad [S_{10}^1]=[S_5^{-1}].
\end{cases}
\tag{46}
$$

In classical elasticity theory the laminated composite shell is modeled using Two-Dimensional plane approximation of the layers, and the forces are considered in the mid-surface. We apply normal forces in the α and β direction which are denoted by $N_{\alpha\alpha}$ and $N_{\beta\beta}$, respectively, and shear forces $N_{\alpha\beta}$. Likewise, we apply moments in the α and β direction which are denoted by $M_{\alpha\alpha}$, $M^*_{\alpha\alpha}$ and $M_{\beta\beta}$, $M^*_{\beta\beta}$ respectively, and torsional moments $M_{\alpha\beta}$ and $M^*_{\alpha\beta}$.

A shear stress or shear force is defined as a stress which is applied parallel or tangential to the face of material, as opposed to a normal stress which is applied perpendicularly.
In this work, the laminated composite shell is modeled using Three-Dimensional approximation, and the forces are considered in the surface-plane and transverse-plane.
We apply transverse forces in the $1z$, $2z$, and z direction which denoted by S_{1z}, S_{2z} and S_{3z}, respectively (Thus the mechanical load consists to apply only the transverse load). Now we can find the plane-displacements (e, K, Q) and transverse displacement or stretching displacement through thickness $(\overline{q})$ in all the structures necessary for evaluating of three-Dimensional stress and strains components of laminated shell. Any condition is used on the choice of $\overline{q}$. The developed 3D laminated constitutive relations account all the coupling terms related to thickness variation during the deformation and section warping. A variation of thickness during the deformation produces a transversal distortion and produces therefore the transverse shear.

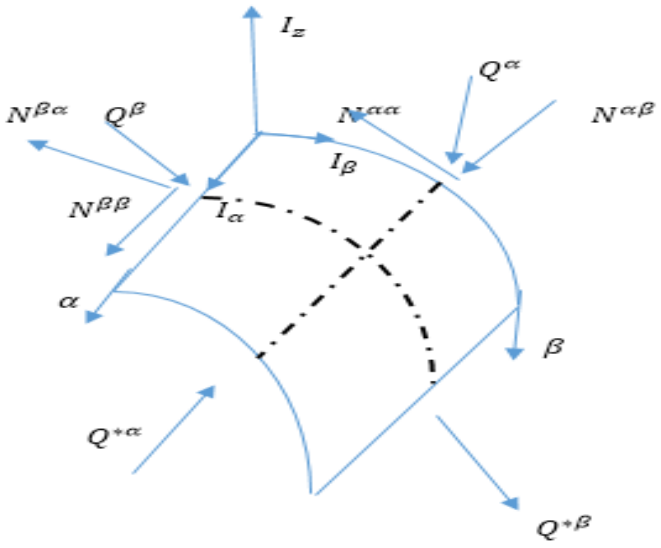

Figure 3: Forces, bending moments and Gauss moments in curvilinear coordinates on mid-surface.

4 Derivation of 3D laminated shell motion equations in curvilinear accounting the new mechanical couplings

The displacement components at any point in the shell read [26]:

$$\begin{cases} U_1(\mathbf{x},z,t) = u_1(\mathbf{x},t) - z\beta_1(\mathbf{x},t) + z^2\Phi_1(\mathbf{x},t), \\ U_2(\mathbf{x},z,t) = u_2(\mathbf{x},t) - z\beta_2(\mathbf{x},t) + z^2\Phi_2(\mathbf{x},t), \\ U_3(\mathbf{x},z,t) = u_3(\mathbf{x},t) + q(\mathbf{x},z,t). \end{cases} \tag{47}$$

The micro-mechanical behavior obtained by this dynamical kinematic is derived as in (27) and static the deformation tensors $\mathbf{e}_{\alpha\beta}(\widetilde{u}(\mathbf{x}))$, $\mathbf{K}_{\alpha\beta}(\widetilde{u}(\mathbf{x}))$, $\mathbf{Q}_{\alpha\beta}(\widetilde{u}(\mathbf{x}))$ and $q(\mathbf{x})\Upsilon_{\alpha\beta}$ are replaced by the dynamic tensors: $\mathbf{e}_{\alpha\beta}(\widetilde{u}(\mathbf{x},t))$, $\mathbf{K}_{\alpha\beta}(\widetilde{u}(\mathbf{x},t))$, $\mathbf{Q}_{\alpha\beta}(\widetilde{u}(\mathbf{x},t))$ and $q(\mathbf{x},t)\Upsilon_{\alpha\beta}$.

4.1 Hamilton's principle for the composite materials

We Consider here a cross-ply laminated composite doubly curved shallow shell panel in coordinate (α,β,z), as shown in Fig.3; symbol such that a, b,and h are dimensions of the shell in the $\alpha-direction$, $\beta-direction$, and thickness of the shell, respectively. Using three-dimensional shell theory we have developed a motion equation by using Hamilton's principle(or the dynamic version of the principle of virtual displacements). we obtained the following equation:

$$\int_0^T \delta L dt = \int_0^T \left[\delta K - (\delta U - \delta P)\right] dt = 0, \tag{48}$$

where δ, δK, δU and δP denote the variational symbol, the virtual kinetic energy, the virtual strain energy, and the virtual potential energy of the external laterally distributed load on the shell respectively.

The finding of virtual kinetic energy, virtual strain energy and virtual potential energy remain open problem for some shell theories no mathematical justified. A such situation can lead to system of equation no clear and no funded physically. Here, we present a rigorous derivation of dynamic equations for a thick laminated shell accounting the general composite coefficients.

$$
\begin{aligned}
\delta K &= \int_V \rho(\dot{U}_\alpha \delta\dot{U}_\alpha + \dot{U}_3\delta\dot{U}_3)dV \qquad (49)\\
&= \int_S\int_{-\frac{h}{2}}^{\frac{h}{2}} \rho\left[(\dot{u}_\alpha - z\dot{\beta}_\alpha + z^2\dot{\Phi}_\alpha)(\delta\dot{u}_\alpha - z\delta\dot{\beta}_\alpha + z^2\delta\dot{\Phi}_\alpha) + \dot{u}_3\delta\dot{u}_3 + \dot{y}\delta\dot{y}\right] A_\alpha A_\beta d\alpha d\beta dz\\
&= \int_S \left[I_0(\dot{u}_\alpha\delta\dot{u}_\alpha + \dot{u}_3\delta\dot{u}_3) - I_1(\dot{u}_\alpha\dot{\theta}_\alpha + \dot{\beta}_\alpha\delta\dot{u}_\alpha + \dot{\overline{y}}\delta\dot{\overline{y}}) + I_2(\dot{u}_\alpha\delta\dot{\Phi}_\alpha + \dot{\beta}_\alpha\delta\dot{\beta}_\alpha + \dot{u}_\alpha\dot{\Phi}_\alpha\delta\dot{u}_\alpha)\right] A_\alpha A_\beta d\alpha d\beta\\
&- \int_S \left[I_3(\dot{\beta}_\alpha\dot{\Phi}_\alpha + \dot{\Phi}_\alpha\delta\dot{\beta}_\alpha) + I_4\dot{\Phi}_\alpha\delta\dot{\Phi}_\alpha\right] A_\alpha A_\beta d\alpha d\beta\\
&= \int_S \left[(I_0\dot{u}_\alpha - I_1\dot{\beta}_\alpha + I_2\dot{\Phi}_\alpha)\delta\dot{u}_\alpha + (-I_1\dot{u}_\alpha + I_2\dot{\beta}_\alpha - I_3\dot{\Phi}_\alpha)\delta\dot{\beta}_\alpha\right] A_\alpha A_\beta d\alpha d\beta\\
&+ \int_S \left[(I_2\dot{u}_\alpha - I_3\dot{\theta}_\alpha + I_4\dot{\Phi}_\alpha)\delta\dot{\Phi}_\alpha + I_0\dot{u}_3\delta\dot{u}_3 - I_1\dot{\overline{y}}\delta\dot{\overline{y}}\right] A_\alpha A_\beta d\alpha d\beta\\
&= -\int_0^T\int_S \left[(I_0\ddot{u}_\alpha - I_1\ddot{\theta}_\alpha + I_2\ddot{\Phi}_\alpha)\delta u_\alpha + (-I_1\ddot{u}_\alpha + I_2\ddot{\beta}_\alpha - I_3\ddot{\Phi}_\alpha)\delta\beta_\alpha\right] A_\alpha A_\beta d\alpha d\beta dt\\
&+ \int_0^T\int_S \left[(I_2\ddot{u}_\alpha - I_3\ddot{\theta}_\alpha + I_4\ddot{\Phi}_\alpha)\delta\Phi_\alpha + I_0\ddot{u}_3\delta u_3 - I_1\ddot{\overline{y}}\delta\overline{y}\right] A_\alpha A_\beta d\alpha d\beta dt\\
&+ \int_S \left[(I_0\dot{u}_\alpha - I_1\dot{\beta}_\alpha + I_2\dot{\Phi}_\alpha)\delta u_\alpha + (-I_1\dot{u}_\alpha + I_2\dot{\beta}_\alpha - I_3\dot{\Phi}_\alpha)\delta\beta_\alpha\right]_0^T A_\alpha A_\beta d\alpha d\beta\\
&+ \int_S \left[(I_2\dot{u}_\alpha - I_3\dot{\beta}_\alpha + I_4\dot{\Phi}_\alpha)\delta\Phi_\alpha + I_0\dot{u}_3\delta u_3 + I_1\ddot{\overline{y}}\delta\overline{y}\right]_0^T A_\alpha A_\beta d\alpha d\beta,
\end{aligned}
$$

where $I_i = \int_{-\frac{h}{2}}^{\frac{h}{2}} \rho z^i dz$ are the mass inertias, ρ is the mass density,V is the shell volume, and S is the inner surface. dV and dS values depend on geometric shell. The virtual strain energy is derived as follows:

$$
\begin{aligned}
\delta U &= \int_V \sigma^{ij}\delta\epsilon_{ij}dV = \int_S\int_{-\frac{h}{2}}^{\frac{h}{2}} (\sigma^{\alpha\beta}\delta\epsilon_{\alpha\beta} + \int_S\int_{-\frac{h}{2}}^{\frac{h}{2}} \sigma^{\alpha 3}\delta\epsilon_{\alpha 3} + \int_S\int_{-\frac{h}{2}}^{\frac{h}{2}} \sigma^{33}\delta\epsilon_{33}) A_\alpha A_\beta d\alpha d\beta dz \qquad (50)\\
&= \int_w \left(N^{\alpha\beta}\delta e_{\alpha\beta}(\bar{v}) + M^{\alpha\beta}\delta K_{\alpha\beta}(\bar{v}) + M^{*\alpha\beta}\delta Q_{\alpha\beta}(\bar{v}) + \mathcal{S}^{\alpha\beta}\delta(\Upsilon_{\alpha\beta}\overline{q})\right) A_\alpha A_\beta d\alpha d\beta \qquad (51)\\
&+ \int_S \left(\mathcal{S}^{\alpha 3}\delta(\nabla_\alpha q) + \mathcal{S}^{33}\delta\overline{q}\right) A_\alpha A_\beta d\alpha d\beta
\end{aligned}
$$

The virtual speed of deformation, the virtual speed of curvature variation, the virtual speed of gauss curvature and the virtual speed of stretching deformation are defined by:

$$
\begin{aligned}
\delta e_{\alpha\beta}(\bar{v}) &= \frac{1}{2}(\nabla_\alpha\delta\eta_\beta + \nabla_\alpha\delta\eta_\alpha - 2b_{\alpha\beta}\delta u_3) = \nabla_\alpha\delta\eta_\beta - b_{\alpha\beta}\delta\eta_3 \qquad (52)\\
\delta K_{\alpha\beta}(\bar{v}) &= \nabla_\alpha(\nabla_\beta\delta\eta_3 + b^\rho_\beta\delta\eta_\rho) + b^\rho_\alpha(\nabla\nabla_\beta\delta\eta_\rho - b_{\beta\rho}\delta\eta_3) \qquad (53)\\
\delta Q_{\alpha\beta}(\bar{v}) &= \frac{1}{2}(b^\rho_\alpha\nabla_\beta(b^\gamma_\rho\delta\eta_\rho + \nabla_\rho\delta\eta_3) + b^\rho_\alpha\nabla_\alpha(b^\gamma_\rho\delta\eta_\gamma + \nabla_\rho\delta\eta_3)) \qquad (54)\\
\delta(\Upsilon_{\alpha\beta}\overline{q}) &= -\frac{1}{2}(\mu^\nu_\alpha b_{\nu\beta} + \mu^\nu_\beta b_{\nu\alpha})\delta\overline{y}\\
\delta(\nabla_\alpha q) &= -\nabla_\alpha\delta\overline{y}
\end{aligned}
$$

Expression of δP for 3D loadings

Now we give the expression of δP for 3D loadings. We have the following kinematic reformulation:

$$\begin{aligned} U_\alpha &= u_\alpha(\alpha,\beta) - z(\nabla_\alpha u_3 + 2b^\tau_\alpha u_\tau) + z^2(b^\lambda_\lambda b^\tau_\alpha u_\tau + b^\tau_\alpha \nabla_\alpha u_3), \qquad (55)\\ &= u_\alpha(\alpha,\beta) - z\beta_\alpha(\alpha,\beta) + z^2\Psi_\alpha(\alpha,\beta),\\ &= w^\rho_\alpha(z)u_\rho + \bar{w}^\rho_\alpha(z)\nabla_\rho u_3 - zb^\rho_\alpha u_\rho\\ &= u_\alpha - z(\theta_\alpha + b^\rho_\alpha u_\rho) - z^2\theta_\alpha b^\rho_\alpha, \qquad (56)\\ U_3 &= u_3(\alpha,\beta) + q(\mathbf{x},z), \end{aligned}$$

where $w^\rho_\alpha(z) = \delta^\rho_\alpha - zb^\rho_\alpha + z^2 b^\lambda_\lambda b^\tau_\alpha$; $\bar{w}^\rho_\alpha(z) = -z\delta^\rho_\alpha + z^2 b^\rho_\tau$; $\theta_\alpha = -(\nabla_\alpha u_3 + b^\rho_\alpha u_\rho)$; $\beta_\alpha(\alpha,\beta) = \nabla_\alpha u_3 + 2b^\tau_\alpha u_\tau$; and the thickness coordinate $z \in \left]-\frac{h}{2},\frac{h}{2}\right[$.

Shell construction

Let the border of S, $\partial S = \gamma_0 \cup \gamma_1$, be partitioned in two parts and the border of the shell $\partial\Omega = \Gamma_0 \cup \Gamma_1$ with $\Gamma_0 = \gamma_0 \times \left]-\frac{h}{2},\frac{h}{2}\right[$, and $\Gamma_0 = \gamma_1 \times \left]-\frac{h}{2},\frac{h}{2}\right[\cup \Gamma_- \cup \Gamma_+$ we denote $\Gamma_- = S \times \{-\frac{h}{2}\}$ and $\Gamma_+ = S \times \{+\frac{h}{2}\}$. Consider a laminated composite shell of thickness h, clamped on part of its border Γ_0, and subject to volume forces f^α and f^3 and to surface forces $\tilde{g}^\alpha$ and $\tilde{g}^3$ on the rest of its border Γ_1.

Virtual potential energy

Let us $\bar{v} = (\bar{v}_\alpha, \bar{v}_3) = (\eta_\rho, \eta_3)$. One has:

$$
\begin{aligned}
\delta P &= \int_\Omega f\delta\bar{v}dX + \int_\Gamma g\delta\bar{v}d\Gamma \qquad (57)\\
&= \int_S\int_{-\frac{h}{2}}^{\frac{h}{2}} f^\alpha\delta\bar{v}_\alpha dSdz + \int_S\int_{-\frac{h}{2}}^{\frac{h}{2}} f^3\delta\bar{v}_3 dSdz + \int_{\Gamma_1} g^\alpha\delta\bar{v}_\alpha d\Gamma + \int_{\Gamma_1} g^3\delta\bar{v}_3 d\Gamma\\
&= \int_S\int_{-\frac{h}{2}}^{\frac{h}{2}} f^\alpha\delta\bar{v}_\alpha dSdz + \int_S\int_{-\frac{h}{2}}^{\frac{h}{2}} f^\alpha\delta\bar{v}_\alpha dSdz + \int_S\int_{-\frac{h}{2}}^{\frac{h}{2}} f^3 dz\delta\eta_3 dS + \int_S\int_{-\frac{h}{2}}^{\frac{h}{2}} f^3 w(z)dz\delta\overline{y}dS + \int_{S\times\{-\frac{h}{2}\}} g^\alpha\delta\bar{v}_\alpha dS\\
&+ \int_{S\times\{\frac{h}{2}\}} g^\alpha\delta\bar{v}_\alpha dS + \int_{\gamma_1}\int_{-\frac{h}{2}}^{\frac{h}{2}} g^\alpha\delta\bar{v}_\alpha dzd\gamma + \int_{S\times\{\frac{h}{2}\}} g^3\delta\eta_3 ds + \int_{S\times\{-\frac{h}{2}\}} g^3\delta\eta_3 ds + \int_{\gamma_1}\int_{-\frac{h}{2}}^{\frac{h}{2}} g^3\delta\eta_3 dzd\gamma\\
&+ \int_{S\times\{\frac{h}{2}\}} g^3 w(z)\delta\overline{y}dS + \int_{S\times\{-\frac{h}{2}\}} g^3 w(z)\delta\overline{y}dS + \int_{\gamma_1}\int_{-\frac{h}{2}}^{\frac{h}{2}} g^3 w(z)\delta\overline{y}dzd\gamma\\
&= \int_S\int_{-\frac{h}{2}}^{\frac{h}{2}} f^\alpha w^\rho_\alpha(z)\delta\eta_\rho dSdz + \int_S\int_{-\frac{h}{2}}^{\frac{h}{2}} f^\alpha\bar{w}^\rho_\alpha(z)\delta\nabla\delta\eta_3 dSdz - \int_S\int_{-\frac{h}{2}}^{\frac{h}{2}} f^\alpha z b^\rho_\alpha dz\delta\eta_\rho dS\\
&+ \int_S\int_{-\frac{h}{2}}^{\frac{h}{2}} f^3\delta\eta_3 dSdz + \int_{S\times\{-\frac{h}{2}\}} g^\alpha\left(w^\rho_\alpha(z)\delta\eta_\rho + \bar{w}^\rho_\alpha(z)\nabla_\rho\delta\eta_3 - z b^\rho_\alpha\delta\eta_\rho\right)dS\\
&+ \int_{S\times\{\frac{h}{2}\}} g^\alpha\left(w^\rho_\alpha(z)\delta\eta_\rho + \bar{w}^\rho_\alpha(z)\nabla_\rho\delta\eta_3 - z b^\rho_\alpha\delta\eta_\rho\right)dS + + \int_{\gamma_1}\int_{-\frac{h}{2}}^{\frac{h}{2}} g^3 w(z)\delta\overline{y}dzd\gamma\\
&+ \int_{\gamma_1}\int_{-\frac{h}{2}}^{\frac{h}{2}} g^\alpha\left(\delta\eta_\alpha - z(\delta\theta_\alpha + b^\rho_\alpha\delta\eta_\rho) - z^2\delta\theta_\rho b^\rho_\alpha\right) + \int_{S\times\{\frac{h}{2}\}} g^3 w(z)\delta\overline{y}dS + \int_{S\times\{-\frac{h}{2}\}} g^3 w(z)\delta\overline{y}dS\\
&= \int_S\left(\int_{-\frac{h}{2}}^{\frac{h}{2}} f^\alpha w^\rho_\alpha(z)dz\right)\delta\eta_\rho dS + \int_S\partial_\rho\left(\int_{-\frac{h}{2}}^{\frac{h}{2}} f^\alpha\bar{w}^\rho_\alpha(z)dz\right)\delta\eta_3 dS + \int_S\int_{-\frac{h}{2}}^{\frac{h}{2}} f^3 dz\delta\eta_3 dS + \int_S\int_{-\frac{h}{2}}^{\frac{h}{2}} w(z)f^3 dz\delta\overline{y}dS\\
&- \int_S\partial_\rho\left(\int_{-\frac{h}{2}}^{\frac{h}{2}}\tilde{g}^\tau_-\bar{w}^\rho_\alpha(-\frac{h}{2}) + \tilde{g}^\tau_+\bar{w}^\rho_\alpha(\frac{h}{2})dz\right)\delta\eta_3 dS + \int_{\gamma_1}\left(\int_{-\frac{h}{2}}^{\frac{h}{2}}(\tilde{g}^\tau - z b^\alpha_\rho\tilde{g}^\rho)dz\right)\delta\eta_\alpha d\gamma\\
&+ \int_{\gamma_1}\left(\int_{-\frac{h}{2}}^{\frac{h}{2}}(z\tilde{g}^\tau - z^2 b^\alpha_\rho\tilde{g}^\rho)dz\right)\delta\theta_\alpha d\gamma + \int_S\left((\tilde{g}^3_-(-\frac{h}{2}) + \tilde{g}^3_+(\frac{h}{2}))\right)\delta\eta_3 dS\\
&+ \int_S\left((W(-\frac{h}{2})\tilde{g}^3_-(-\frac{h}{2}) + W(\frac{h}{2})\tilde{g}^3_+(\frac{h}{2})\right)\delta\overline{y}dS\int_{\gamma_1}\left(\int_{-\frac{h}{2}}^{\frac{h}{2}}\tilde{g}^3 dz\right)\delta\eta_3 d\gamma + \int_{\gamma_1}\left(\int_{-\frac{h}{2}}^{\frac{h}{2}} w(z)\tilde{g}^3 dz\right)\delta\overline{y}d\gamma\\
&= \int_S[p^\alpha\delta\eta_\alpha + p^3\delta\eta_3 + p^4\delta\overline{y}]dS + \int_{\gamma_1}[q^\alpha\eta_\alpha + q^3\delta\eta_3 + q^4\delta\overline{y}]d\gamma + \int_{\gamma_1} m^\alpha\delta\theta_\alpha d\gamma
\end{aligned}
$$

where

$$
\begin{aligned}
p^\alpha &= \int_{-\frac{h}{2}}^{\frac{h}{2}} f^\alpha w_\alpha^\rho(z)dz + \tilde{g}_-^\tau \bar{w}_\alpha^\rho(-\frac{h}{2}) + \tilde{g}_+^\tau \bar{w}_\alpha^\rho(\frac{h}{2}) \qquad (58)\\
p^3 &= \int_{-\frac{h}{2}}^{\frac{h}{2}} f^3 dz + \tilde{g}_-^3(-\frac{h}{2}) + \tilde{g}_+^3(\frac{h}{2}) - \partial_\rho \left(\int_{-\frac{h}{2}}^{\frac{h}{2}} f^\alpha \bar{w}_\alpha^\rho(z)dz + \tilde{g}_-^\tau \bar{w}_\alpha^\rho(-\frac{h}{2}) + \tilde{g}_+^\tau \bar{w}_\alpha^\rho(\frac{h}{2}) \right)\\
p^4 &= \int_{-\frac{h}{2}}^{\frac{h}{2}} w(z) f^3 dz + W(-\frac{h}{2})\tilde{g}_-^3(-\frac{h}{2}) + W(\frac{h}{2})\tilde{g}_+^3(\frac{h}{2})\\
q^\alpha &= \int_{-\frac{h}{2}}^{\frac{h}{2}} \left(\tilde{g}^\tau - z b_\rho^\alpha \tilde{g}^\rho\right) dz\\
q^3 &= \int_{-\frac{h}{2}}^{\frac{h}{2}} \tilde{g}^3 dz\\
q^4 &= \int_{-\frac{h}{2}}^{\frac{h}{2}} w(z)\tilde{g}^3 dz\\
m^\alpha &= \int_{-\frac{h}{2}}^{\frac{h}{2}} (z\tilde{g}^\tau - z^2 b_\rho^\alpha \tilde{g}^\rho) dz
\end{aligned}
$$

.

In Eqs.(57)-(58), q^α, q^3 are the line load. $m = m^\alpha A^\alpha$ are the linear density moment obtained on the free contour γ that contains the forces on Γ_1 take on S. In fact, we have $m = m^\alpha A^\alpha = m^\nu \vec{\nu} + m^t \vec{t}$, where m^t and m^ν are the bending density moments and the twistong density moments applied on γ_1. The coupled moment

$$m^\alpha \theta_\alpha = m^t \theta_\nu - m^\nu \theta_t = m^t \theta_\nu + m^\nu \vec{n}.\partial_t v \qquad (59)$$

where $m^t = m.\vec{t}$, $m^\nu = m.\vec{\nu}$ work on the angle due to the variation of $\vec{\nu}$ while m^ν work on the angle to variation of $\vec{t}$. Using the fact that $\partial_{\vec{t}} = t^\alpha \partial_\alpha$, $\partial_{\vec{n}} v_\alpha = B_\alpha^\rho A_\rho$, $\vec{n}.v = v_3$ and $m^\nu \vec{n}.\partial_t v = -\partial_t m^\nu \vec{n}.v - m^\nu \partial_t \vec{n}.v$. We can show easily that the term $\int_{\gamma_1} m^\alpha \delta\theta_\alpha d\gamma$ in (57):

$$\int_{\gamma_1} m^\alpha \delta\theta_\alpha d\gamma = \int_{\gamma_1} \left(m^t \delta\theta_\nu - \partial_{\vec{t}} m^\nu \delta v_3 + m^\nu t_\alpha B_\alpha^\rho \delta v_\rho \right) d\gamma \qquad (60)$$

4.2 The motion equations and boundary conditions

Here, we derive using Hamilton's principle given by (48), a system of equations that describes the dynamic motion of the 3D laminated shell under loading computed previously (see Eq.(58)). This system reads:

$$\begin{cases}
\dfrac{\partial(A_\beta N^{\alpha\alpha})}{\partial\alpha}+\dfrac{\partial(A_\alpha N^{\alpha\beta})}{\partial\beta}+\dfrac{\partial A_\alpha}{\partial\beta}N^{\alpha\beta}-\dfrac{\partial A_\beta}{\partial\alpha}N^{\beta\beta}+\dfrac{1}{2}\dfrac{\partial(A_\beta\mathcal{S}^{13})}{\partial\alpha}-\dfrac{A_\alpha A_\beta Q^\alpha}{R_\alpha}-\dfrac{A_\alpha A_\beta Q^{*\alpha}}{R_\alpha^2}\\
+p^\alpha=A_\alpha A_\beta\left(I_0\ddot{u}-I_1\ddot{\beta}_1+I_2\ddot{\Phi}_1\right)\\
\dfrac{\partial(A_\beta N^{\alpha\beta})}{\partial\alpha}+\dfrac{\partial(A_\alpha N^{\beta\beta})}{\partial\beta}+\dfrac{\partial A_\beta}{\partial\alpha}N^{\alpha\beta}-\dfrac{\partial A_\alpha}{\partial\beta}N^{\alpha\alpha}+\dfrac{1}{2}\dfrac{\partial(A_\alpha\mathcal{S}^{23})}{\partial\beta}-\dfrac{A_\alpha A_\beta Q^\beta}{R_\beta}-\dfrac{A_\alpha A_\beta Q^{*\beta}}{R_\beta^2}\\
+p^\beta=A_\alpha A_\beta\left(I_0\ddot{v}-I_1\ddot{\beta}_2+I_2\ddot{\Phi}_2\right)\\
\dfrac{\partial(A_\beta Q^\alpha)}{\partial\alpha}+\dfrac{\partial(A_\alpha Q^\alpha)}{\partial\beta}-A_\alpha A_\beta\left(\dfrac{N^{\alpha\alpha}}{R_\alpha}+\dfrac{N^{\beta\beta}}{R_\beta}\right)+\dfrac{A_\alpha A_\beta M^{\beta\beta}}{R_\beta^2}+\dfrac{A_\alpha A_\beta M^{\alpha\alpha}}{R_\alpha^2}+\dfrac{1}{R_\alpha}\dfrac{\partial(A_\beta Q^{*\alpha})}{\partial\alpha}\\
+\dfrac{1}{R_\beta}\dfrac{\partial(A_\alpha Q^{*\beta})}{\partial\alpha}+p^3=A_\alpha A_\beta I_0\ddot{u}_3\\
\dfrac{1}{2}\mathcal{S}^{\alpha\alpha}\left(\dfrac{1}{R_\alpha}+\dfrac{1}{R_\beta}\right)+A_\alpha A_\beta\dfrac{1}{2}\mathcal{S}^{\beta\beta}\left(\dfrac{1}{R_\alpha}+\dfrac{1}{R_\beta}\right)+\dfrac{1}{2}\dfrac{\partial(A_\beta\mathcal{S}^{13})}{\partial\alpha}+\dfrac{1}{2}\dfrac{\partial(A_\alpha\mathcal{S}^{23})}{\partial\beta}+\dfrac{\partial(A_\alpha A_\beta\mathcal{S}^{33})}{\partial z}+p^4=-A_\alpha A_\beta I_1\ddot{q}\\
\dfrac{\partial(A_\beta M^{\alpha\alpha})}{\partial\alpha}-\dfrac{\partial A_\beta}{\partial\alpha}M^{\alpha\beta}+\dfrac{\partial(A_\alpha M^{\beta\alpha})}{\partial\beta}+\dfrac{\partial A_\alpha}{\partial\beta}M^{\alpha\beta}-A_\alpha A_\beta Q^\alpha+A_\alpha A_\beta m_\alpha=A_\alpha A_\beta\left(-I_1\ddot{u}\right)+I_2\ddot{\theta}_1-I_3\ddot{\Phi}_1\\
\dfrac{\partial(A_\beta M^{\alpha\beta})}{\partial\alpha}+\dfrac{\partial A_\beta}{\partial\alpha}M^{\beta\alpha}+\dfrac{\partial(A_\alpha M^{\beta\beta})}{\partial\beta}-\dfrac{\partial A_\alpha}{\partial\beta}M^{\alpha\alpha}-A_\alpha A_\beta Q^\beta+A_\alpha A_\beta m_\beta=A_\alpha A_\beta\left(-I_1\ddot{v}+I_2\ddot{\beta}_2-I_3\ddot{\Phi}_2\right)\\
\dfrac{\partial(A_\beta M^{*\alpha\alpha})}{\partial\alpha}-\dfrac{\partial A_\beta}{\partial\alpha}M^{*\alpha\beta}+\dfrac{\partial(A_\alpha M^{*\beta\alpha})}{\partial\beta}+\dfrac{\partial A_\alpha}{\partial\beta}M^{*\alpha\beta}-A_\alpha A_\beta Q^{*\alpha}=A_\alpha A_\beta\left(I_2\ddot{u}-I_3\ddot{\beta}_1+I_4\ddot{\Phi}_1\right)\\
\dfrac{\partial(A_\beta M^{*\alpha\beta})}{\partial\alpha}+\dfrac{\partial A_\beta}{\partial\alpha}M^{*\beta\alpha}+\dfrac{\partial(A_\alpha M^{*\beta\beta})}{\partial\beta}-\dfrac{\partial A_\alpha}{\partial\beta}M^{*\alpha\alpha}-A_\alpha A_\beta Q^{*\beta}=A_\alpha A_\beta\left(I_2\ddot{v}-I_3\ddot{\beta}_2+I_4\ddot{\Phi}_2\right)
\end{cases}\tag{61}$$

We obtain the two-dimensional static and transient behavior of LCS when the terms dependent of q disappears [22].

Boundary conditions

The effect of stretching-through-the-thickness modifies the boundary condition given for 2D case in [22]. Here the equations on the boundaries are given by:

$$\begin{cases}
N^{\alpha\nu}+M^{\nu\nu}b_\nu^\alpha+(2M^{\nu t}+M^{*\nu t}-m^\nu)b_t^\alpha-q^\alpha=0,\\
Q^\nu+Q^{*\nu}-\partial_s(m^\nu-M^{\nu t}-M^{*\nu t})-q^3=0,\\
\mathcal{S}^{\nu 3}-q^4=0,\\
M^{\nu\nu}+M^{*\nu\nu}+m^s=0.
\end{cases}\tag{62}$$

We choice a direct landmark(t,ν,a_n). Note that in many applications of laminated shell structure, we have $m^\nu=0$(moment normal axe on border) where $m^s=m.\nu$ and $m^\nu=m.t$ are the density moments.
On the clamped border γ_1 we have

$$\partial_\nu u_\alpha=0,\quad \partial_\nu w=0,\quad u_\alpha=0,\quad w=0;\ \ \partial_\nu\overline{q}=0;\overline{q}=0.\tag{63}$$

The Three-dimensional motion equation (61) can be written in terms of 3D displacements $(u,v,w,\overline{q},\beta_1,\beta_2,\Phi_1,\Phi_2)$

using the following relations according to 3D constitutive relation for cross-ply symmetric laminates:

$$\begin{cases} N^{\alpha\alpha} = A_{11}u_{,\alpha} + A_{12}\left(\frac{1}{R}(v_{,\beta}+w)\right) - B_{11}w_{,\alpha\alpha} + C_{12}\left(-\frac{1}{R^3}(v_{,\beta}-w_{,\beta\beta})\right) \\ N^{\beta\beta} = A_{12}u_{,\alpha} + A_{22}\left(\frac{1}{R}(v_{,\beta}+w)\right) + B_{11}\left(-\frac{1}{R^2}(2v_{,\beta}-w_{,\beta\beta})\right) + C_{22}\left(-\frac{1}{R^3}(v_{,\beta}-w_{,\beta\beta})\right) \\ N^{\alpha\beta} = 2A_{66}\left(\frac{1}{R}u_{,\beta}+v_{,\alpha}\right) + 2C_{66}\left(-\frac{1}{R^2}(v_{,\alpha}+w_{,\alpha\beta}\right) \\ M^{\alpha\alpha} = -B_{11}u_{,\alpha} + C_{11}w_{,\alpha\alpha} + C_{12}\left(\frac{1}{R^2}(2v_{,\beta}-w_{,\beta\beta})\right) \\ M^{\beta\beta} = B_{11}\left(\frac{1}{R}(v_{,\beta}+w)\right) + C_{12}w_{,\alpha\alpha} + C_{22}\left(-\frac{1}{R^2}(2v_{,\beta}-w_{,\beta\beta})\right) + D_{11}\left(\frac{1}{R^3}(v_{,\beta}-w_{,\beta\beta})\right) \\ M^{\alpha\beta} = 2C_{66}\left(-\frac{1}{R}(v_{,\alpha}-w_{,\alpha\beta}\right) \\ M^{*\alpha\alpha} = C_{11}u_{,\alpha} + C_{12}\left(\frac{1}{R}(v_{,\beta}+w)\right) - D_{11}w_{,\alpha\alpha} + E_{12}\left(-\frac{1}{R^3}(v_{,\beta}-w_{,\beta\beta})\right) \\ M^{*\beta\beta} = C_{12}u_{,\alpha} + C_{12}\left(\frac{1}{R}(v_{,\beta}+w)\right) + D_{11}\left(\frac{1}{R^3}(2v_{,\beta}-w_{,\beta\beta})\right) + E_{22}\left(-\frac{1}{R^3}(v_{,\beta}-w_{,\beta\beta})\right) \\ M^{*\alpha\beta} = 2C_{66}\left(\frac{1}{R}(v_{,\beta}+w)\right) + 2E_{66}\left(-\frac{1}{R^2}(v_{,\alpha}+w_{,\alpha\beta}\right) \end{cases}$$

Remark 4.1. ***The general three-dimensional exact model***

A general three-dimensional exact model for anisotropic doubly-curved shell proposed here is given by Eq. (45) and Eqs. (61)-(64). This general model is proposed for doubly-curved cross-ply laminated shells with constant radii of curvature and they can easily extended for non constant radii or degenerate into relations for cylindrical panels and plates. Using this model, we propose to study the dynamic and static behavior of laminate using Navier's approach.

4.3 A three-dimensional equation using Navier's method for the transient analysis of laminated shell structures

Using the Equation (61) we obtained for simply supported conditions the Mathematical modelings for analytical solutions for dynamic and static response, in many cases of laminates shells (symmetric balanced,angle-ply, cross-ply, etc.). Towards using the Navier type solutions [2], we write the equation of motion (61) in terms of displacements $(u, v, w, \overline{q})$ (as for the 2D case above) by substituting for the plane forces, transverse forces and moments resultant from equation (45) and the equation given by (64) into Equation (61). In the Navier method the generalized displacements are expanded in a double trigonometric series in terms of unknown parameters. The choice of the functions in the series is restricted to those which satisfy the boundary conditions of the problem. When the laminated shell is a simply supported border the mid-surface can turn around the tangent. moreover the reaction $m^s = 0$. The rotation motion around of tangent being free,the

[2]We recall that The Navier solutions were developed for two class of laminates: antisymmetric cross-ply laminates and antisymmetric angle-ply laminates, each for a specific type of simply supported boundary conditions

mathematical expressions for movable simply supported condition are given by:

$$\begin{aligned}
N^{\alpha\alpha} &= N^{\alpha\alpha}(a,\beta,t) = M^{\alpha\alpha}(0,\beta,t) = M^{\alpha\alpha}(a,\beta,t) = M^{*\alpha\alpha}(0,\beta,t) = M^{*\alpha\alpha}(a,\beta,t) \\
&= \mathcal{S}^{\alpha\alpha}(0,\beta,t) = \mathcal{S}^{\alpha\alpha}(a,\beta,t) = 0, \\
u(0,\beta,t) &= u(a,\beta,t) = v(0,\beta,t) = v(a,\beta,t) = w(0,\beta,t) = w(a,\beta,t) = \overline{q}(0,\beta,t) = \overline{q}(a,\beta,t) = 0, \\
N^{\beta\beta}(0,\beta,t) &= N^{\beta\beta}(a,\beta,t) = M^{\beta\beta}(\alpha,0,t) = M^{\beta\beta}(\alpha,b,t) = M^{*\beta\beta}(\alpha,0,t) = M^{*\beta\beta}(\alpha,b,t) \\
&= \mathcal{S}^{\beta\beta}(\alpha,0,t) = \mathcal{S}^{\beta\beta}(\alpha,b,t) = 0, \\
u(\alpha,0,t) &= u(\alpha,b,t) = v(\alpha,0,t) = v(\alpha,b,t) = w(\alpha,0,t) = w(\alpha,b,t) = \overline{q}(\alpha,0,t) = \overline{q}(\alpha,b,t) = 0, \\
\theta_2(0,\beta,t) &= \theta_2(a,\beta,t) = \theta_1(\alpha,0,t) = \theta_1(\alpha,b,t) = 0, \\
\Phi_2(0,\beta,t) &= \Phi_2(a,\beta,t) = \Phi_1(\alpha,0,t) = \Phi_1(\alpha,b,t) = 0,
\end{aligned} \tag{64}$$

Following the state space technique, we assume the following solution form that satisfies the boundary condition in Equations(64)

$$\begin{cases}
u(x,y,t) = \sum_{m,n=1}^{\infty} U_{mn}(t)\cos\hat{\alpha}x\sin\hat{\beta}y \\
v(x,y,t) = \sum_{m,n=1}^{\infty} V_{mn}(t)\sin\hat{\alpha}x\cos\hat{\beta}y \\
w(x,y,t) = \sum_{m,n=1}^{\infty} W_{mn}(t)\sin\hat{\alpha}x\sin\hat{\beta}y \\
\overline{q}(x,y,t) = \sum_{m,n=1}^{\infty} \overline{Q}_{mn}(t)\sin\hat{\alpha}x\sin\hat{\beta}y \\
\theta_1(x,y,t) = \sum_{m,n=1}^{\infty} \theta_{1mn}(t)\cos\hat{\alpha}x\sin\hat{\beta}y \\
\theta_2(x,y,t) = \sum_{m,n=1}^{\infty} \theta_{2mn}(t)\sin\hat{\alpha}x\cos\hat{\beta}y \\
\Phi_1(x,y,t) = \sum_{m,n=1}^{\infty} \Phi_{1mn}(t)\cos\hat{\alpha}x\sin\hat{\beta}y \\
\Phi_2(x,y,t) = \sum_{m,n=1}^{\infty} \Phi_{2mn}(t)\sin\hat{\alpha}x\cos\hat{\beta}y
\end{cases} \tag{65}$$

where U_{mn}, V_{mn}, $W_{mn}, \overline{Q}_{mn}$ θ_{1mn}, θ_{2mn}, Φ_{1mn}, Φ_{2mn} are the coefficient . $\hat{\alpha} = \frac{m\pi}{a}$; $\hat{\beta} = \frac{n\pi}{b}$. The transverse load p^3 is also expanded in double fourier sine series.

$$p^3(x,y,t) = \sum_{m,n=1}^{\infty} P^3_{mn}(t)\sin\hat{\alpha}x\sin\hat{\beta}y \tag{66}$$

where $P^3_{mn}(t) = \frac{4}{ab}\int_0^a\int_0^b p^3(x,y,t)\sin\hat{\alpha}x\sin\hat{\beta}y dxdy$. Substituting Eqs.(65)-(66) into the equilibrium equations with respect to displacement components of Equation (61), it can be obtained as follows

$$[K]\{\Delta t\} + [M]\{\ddot{\Delta} t\} = \{F(t)\} \tag{67}$$

Where $\{\Delta t\}_{8\times1} = \{U_{mn}(t), V_{mn}(t), W_{mn}(t), \overline{Q}_{mn}(t), \theta_{1mn}(t), \theta_{2mn}(t), \Phi_{1mn}(t), \Phi_{2mn}(t)\}^t$;
$\{\ddot{\Delta} t\}_{8\times1} = \{\ddot{U}_{mn}(t), \ddot{V}_{mn}(t), \ddot{W}_{mn}(t), \ddot{\overline{Q}}_{mn}(t), \ddot{\theta}_{1mn}(t), \ddot{\theta}_{2mn}(t), \ddot{\Phi}_{1mn}(t), \ddot{\Phi}_{2mn}(t)\}^t$;
$\{F(t)\}_{8\times1} = \{0, 0, p^3_{mn}(t), 0, 0, 0, 0, 0\}^t$
;

$$
\begin{aligned}
[K]_{8\times 8} &= \begin{pmatrix}
\widehat{S}_{11} & \widehat{S}_{12} & \widehat{S}_{13} & \widehat{S}_{14} & \widehat{S}_{15} & \widehat{S}_{16} & \widehat{S}_{17} & \widehat{S}_{18} \\
q\widehat{S}_{21} & \widehat{S}_{22} & \widehat{S}_{23} & \widehat{S}_{24} & \widehat{S}_{25} & \widehat{S}_{26} & \widehat{S}_{27} & \widehat{S}_{28} \\
\widehat{S}_{31} & \widehat{S}_{32} & \widehat{S}_{33} & \widehat{S}_{34} & \widehat{S}_{35} & \widehat{S}_{36} & \widehat{S}_{37} & \widehat{S}_{38} \\
\widehat{S}_{41} & \widehat{S}_{42} & \widehat{S}_{43} & \widehat{S}_{44} & \widehat{S}_{45} & \widehat{S}_{46} & \widehat{S}_{47} & \widehat{S}_{48} \\
\widehat{S}_{51} & \widehat{S}_{52} & \widehat{S}_{53} & \widehat{S}_{54} & \widehat{S}_{55} & \widehat{S}_{56} & \widehat{S}_{57} & \widehat{S}_{58} \\
\widehat{S}_{61} & \widehat{S}_{62} & \widehat{S}_{63} & \widehat{S}_{64} & \widehat{S}_{65} & \widehat{S}_{66} & \widehat{S}_{67} & \widehat{S}_{68} \\
\widehat{S}_{71} & \widehat{S}_{72} & \widehat{S}_{73} & \widehat{S}_{74} & \widehat{S}_{75} & \widehat{S}_{76} & \widehat{S}_{77} & \widehat{S}_{78} \\
\widehat{S}_{81} & \widehat{S}_{82} & \widehat{S}_{83} & \widehat{S}_{84} & \widehat{S}_{85} & \widehat{S}_{86} & \widehat{S}_{87} & \widehat{S}_{88}
\end{pmatrix} \\
[\widehat{M}]_{8\times 8} &= \begin{pmatrix}
\widehat{M}_{11} & 0 & 0 & 0 & \widehat{M}_{15} & 0 & \widehat{M}_{17} & 0 \\
0 & \widehat{M}_{22} & 0 & 0 & 0 & \widehat{M}_{26} & 0 & \widehat{M}_{28} \\
0 & 0 & \widehat{M}_{33} & 0 & 0 & 0 & 0 & 0 \\
0 & 0 & 0 & \widehat{M}_{44} & 0 & 0 & 0 & 0 \\
\widehat{M}_{51} & 0 & 0 & 0 & \widehat{M}_{55} & 0 & \widehat{M}_{57} & 0 \\
0 & \widehat{M}_{62} & 0 & 0 & 0 & \widehat{M}_{66} & 0 & \widehat{M}_{68} \\
\widehat{M}_{71} & 0 & 0 & 0 & \widehat{M}_{75} & 0 & \widehat{M}_{77} & 0 \\
0 & \widehat{M}_{82} & 0 & 0 & 0 & \widehat{M}_{86} & 0 & \widehat{M}_{88}
\end{pmatrix}
\end{aligned}
\tag{68}
$$

The coefficient of $\widehat{S}$ is given by Equation 69:

$$
\begin{cases}
\widehat{S}_{11} = A_{11}\hat{\alpha}^2 + A_{66}\hat{\beta}^2; \widehat{S}_{12} = (A_{12} + A_{66})\hat{\alpha}\hat{\beta}; \\
\widehat{S}_{13} = (-\frac{A_{11}}{R_\alpha} - \frac{A_{12}}{R_\beta} + \frac{B_{11}}{R_\alpha^2} + \frac{B_{12}}{R_\beta^2})\hat{\alpha}; \\
\widehat{S}_{15} = B_{11}\hat{\alpha}^2 + B_{66}\hat{\beta}^2; \widehat{S}_{16} = (B_{12} + B_{66})\hat{\alpha}\hat{\beta}; \widehat{S}_{17} = C_{11}\hat{\alpha}^2 + C_{66}\hat{\beta}^2; \\
\widehat{S}_{18} = (C_{12} + C_{66})\hat{\alpha}\hat{\beta}; \widehat{S}_{22} = A_{66}\hat{\alpha}^2 + A_{22}\hat{\beta}^2; \\
\widehat{S}_{23} = (-\frac{A_{12}}{R_\alpha} - \frac{A_{22}}{R_\beta} + \frac{B_{12}}{R_\alpha^2} + \frac{B_{22}}{R_\beta^2})\hat{\beta}; \\
S_{25} = (B_{12} + B_{66})\hat{\alpha}\hat{\beta}; \\
\widehat{S}_{26} = B_{22}\hat{\beta}^2 + B_{66}\hat{\alpha}^2; \widehat{S}_{27} = (C_{12} + C_{66})\hat{\alpha}\hat{\beta}; \widehat{S}_{28} = C_{22}\hat{\beta}^2 + C_{66}\hat{\alpha}^2; \\
\widehat{S}_{33} = \frac{A_{11}}{R_\alpha^2} + 2\frac{A_{12}}{R_\alpha R_\beta} + \frac{A_{22}}{R_\beta^2} - (\frac{B_{11}}{R_\alpha^3} + \chi_0 B_{12} + \frac{B_{22}}{R_\beta^3}) + \frac{C_{11}}{R_\alpha^4} + \chi_1 C_{12} + \frac{C_{22}}{R_\beta^4}; \\
\widehat{S}_{35} = (\frac{B_{11}}{R_\alpha} + \frac{B_{12}}{R_\beta} - \frac{C_{11}}{R_\alpha^2} - \frac{C_{12}}{R_\beta^2})\hat{\alpha}; \widehat{S}_{36} = (\frac{B_{22}}{R_\beta} + \frac{B_{12}}{R_\alpha} - \frac{C_{22}}{R_\beta^2} - \frac{C_{12}}{R_\alpha^2})\hat{\alpha}; \\
\widehat{S}_{37} = (-\frac{C_{11}}{R_\alpha} - \frac{C_{12}}{R_\beta} + \frac{D_{11}}{R_\alpha^2} + \frac{D_{12}}{R_\beta^2})\hat{\alpha}; \\
\widehat{S}_{38} = (\frac{C_{22}}{R_\beta} + \frac{C_{12}}{R_\alpha} - \frac{D_{22}}{R_\beta^2} - \frac{D_{12}}{R_\alpha^2})\hat{\beta}; S_{55} = C_{11}\hat{\alpha}^2 + C_{66}\hat{\beta}^2; \widehat{S}_{56} = (C_{12} + C_{66})\hat{\alpha}\hat{\beta}; \\
\widehat{S}_{57} = D_{11}\hat{\alpha}^2 + D_{66}\hat{\beta}^2; \widehat{S}_{58} = (D_{12} + D_{66})\hat{\alpha}\hat{\beta}; \widehat{S}_{65} = C_{66}\hat{\alpha}^2 + C_{22}\hat{\beta}^2; \widehat{S}_{66} = (D_{12} + D_{66})\hat{\alpha}\hat{\beta}; \\
\widehat{S}_{67} = D_{66}\hat{\alpha}^2 + D_{22}\hat{\beta}^2; \widehat{S}_{76} = E_{11}\hat{\alpha}^2 + E_{66}\hat{\beta}^2; \widehat{S}_{77} = (E_{12} + E_{66})\hat{\alpha}\hat{\beta}; \widehat{S}_{88} = E_{66}\hat{\alpha}^2 + E_{22}\hat{\beta}^2; \\
\widehat{S}_{14} = \frac{1}{A_\alpha}\left(\frac{1}{R_\alpha} + \frac{1}{R_\beta}\right)(S_1^{11} + S_1^{12})\hat{\alpha} + \frac{1}{2}S_4^{44}\hat{\alpha}^2 \\
\widehat{S}_{24} = \frac{1}{A_\beta}\left(\frac{1}{R_\alpha} + \frac{1}{R_\beta}\right)(S_1^{11} + S_1^{12}) + \frac{1}{R_\alpha}\left(\frac{1}{R_\beta} + \frac{1}{R_\beta}\right)(S_1^{12} + S_1^{22}) + \frac{1}{2}S_4^{55}\hat{\alpha}^2 \\
\widehat{S}_{34} = \frac{1}{R_\alpha^2}\left(\frac{1}{R_\alpha} + \frac{1}{R_\beta}\right)(S_2^{11} + S_2^{12})\frac{1}{R_\beta^2}\left(\frac{1}{R_\alpha} + \frac{1}{R_\beta}\right)(S_2^{12} + S_2^{22}) \\
-\frac{1}{R_\alpha}\left(\frac{1}{R_\alpha} + \frac{1}{R_\beta}\right)(S_1^{11} + S_1^{12}) - \frac{1}{R_\beta}\left(\frac{1}{R_\alpha} + \frac{1}{R_\beta}\right)(S_1^{12} + S_1^{22}) \\
\widehat{S}_{44} = \frac{S_1^{11}}{R_\alpha^2} + 2\frac{S_1^{12}}{R_\alpha R_\beta} + \frac{S_1^{22}}{R_\beta^2} - (\frac{S_2^{11}}{R_\alpha^3} + \chi_0 S_2^{12} + \frac{S_2^{22}}{R_\beta^3}) + \frac{S_3^{11}}{R_\alpha^4} + \chi_1 S^{12_3} + \frac{S_3^{22}}{R_\beta^4} + \\
\left(\frac{1}{R_\alpha} + \frac{1}{R_\beta}\right)(S_4^{11} + S_4^{12}) + \left(\frac{1}{R_\alpha} + \frac{1}{R_\beta}\right)(S_4^{12} + S_4^{22}) + \frac{1}{2}S_4^{44}\hat{\alpha}^2 + \frac{1}{2}S_4^{55}\hat{\beta}^2; \\
\widehat{S}_{54} = \frac{1}{A_\alpha}\left(\frac{1}{R_\alpha} + \frac{1}{R_\beta}\right)(S_2^{11} + S_2^{12})\hat{\alpha} \\
\widehat{S}_{64} = \frac{1}{A_\beta}\left(\frac{1}{R_\alpha} + \frac{1}{R_\beta}\right)(S_2^{12} + S_2^{22})\hat{\alpha} \\
\widehat{S}_{74} = \frac{1}{A_\alpha}\left(\frac{1}{R_\alpha} + \frac{1}{R_\beta}\right)(S_3^{11} + S_3^{12})\hat{\alpha} \\
\widehat{S}_{84} = \frac{1}{A_\beta}\left(\frac{1}{R_\alpha} + \frac{1}{R_\beta}\right)(S_3^{12} + S_3^{22})\hat{\alpha} \\
M_{ij} = M_{ji}; i, j = 1, ...8 M_{11} = M_{22} = M_{33} = I_0; M_{44} = I_1; \\
M_{15} = M_{26} = M_{51} = M_{52} = I_1; \\
M_{17} = M_{27} = M_{55} = M_{66} = M_{61} = M_{82} = I_2; \\
M_{56} = M_{64} = M_{75} = M_{86} = I_3; M_{77} = M_{88}0 = I_4.
\end{cases}
\tag{69}
$$

Here $U_{mn}, V_{mn}, W_{mn}, \overline{Q}_{mn}, \theta_{1mn}, \theta_{2mn}, \Phi_{1mn}, \Phi_{2mn}$ are the amplitudes of displacements (plane and transverse), plane rotation and Gauss rotation evaluated in α, β, z directions. Coefficients $\hat{\alpha} = \dfrac{m\pi}{a}$; $\hat{\beta} = \dfrac{n\pi}{b}$ include m and n as the half-wave numbers, a and b as the shell dimensions in α and β directions, respectively (all these quantities are calculated at the mid-surface of laminated). R_α and R_β are measured at the reference mid-surface (see Fig. 3) of the multilayered shell. A_α and A_β are evaluated through the thickness direction of the laminated shell using Eq. (61). 3D motion equations are written for spherical shells, they automatically degenerate into 3D motion equations for cylindrical closed/open shells when R_α or R_β is infinite (which means A_α or A_β equals one) and into 2D motion equations for plates when R_α and R_β are infinite (which means

A_α and A_β equal one). These features allow a unified and general formulation valid for all the considered geometries

Remark 4.2. *In this new 3D exact model for analysis of laminated shell given by (67)-(68), the matrices K has new coefficients (S_{i6}, S_{i7}, S_{i8} $i = 1, ..8$) absent in several papers available in the literature and dealing with the 2D/3D exact models the mechanical behavior of laminated shells. These coefficients are linked to the presence of Gauss rotations and stretching-through-the-thickness term which influence the center deflection w and the fundamental frequencies of the multilayered shell. The proposed equations is more general than several 3D exact models based on R-M types first order deformation theory and those based on other multilayer theories recently developed and available in the literature.*

Remark 4.3. *For static analysis, the solution can be obtained by solving the equations resulting from Eq. (67) by setting the time derivative terms to zero. If the transverse load over the surface of shell panel considered is uniformly distributed, we can take* $P^3_{mn} = \dfrac{16P^3_0}{mn\pi^2}$ *, P^3_0 is the intensity of the uniformly distributed load.*

For natural vibration analysis, all applied loads are set to zero, $\{F(t)\} = \{0\}$ and we assume that the periodic solutions in Eq. (65).

5 Numerical results

In this section, all the 3D General composite-shell stiffness coefficients for geometrically thick shells and mathematical modelings for static and dynamic mechanical behavior of laminated shells developed here are assessed via some Benchmark problems available in the literature. To demonstrate the accuracy and effectiveness of the proposed exact models, six tests are considered. In test 1, the obtained results from the proposed exact model will be compared with obtained results from classical FSD models and CLST. In test 2 and test 3, the results from the proposed 3D constitutive relations via an analytical method using the 3D simple algorithm above are presented. These tests are performed to compute the interlaminar stress in the laminated composite shell under transverse loading. In test 4 and test 5 the results from the proposed static and transient exact equations will be compared with obtained results from others models obtained in heuristic way or no. These tests consist to find the deflection and fundamental frequencies of the laminated thick, moderately thick as well as thin composite plates and shells. In the last test (test 6), the results from the proposed state-space based methodology will be compared with the method obtained results from the method proposed by [29](stress function method) and [32](displacement-based approach) for cylindrical isotropic and composite shells.

Simple algorithm for the analytical analysis

When the radii of curvature of the shell is very large i.e. $R_\alpha = R_\beta \to \infty$ (plate shells), it's possible to compute directly using the 2D/3D constitutive relations the strains/stress for each layer The following algorithm is a modified version of that proposed in [14] and widely in the literature. This procedure no use the effect of geometric of the shell and is also used to analyze plate structures.

1. Enter the materials properties ($E_1, E_2, E_3, G_{12}, G_{13}, G_{23}$, ν_{12}, ν_{23}, ν_{13}), the layer number (Nb), the fibre angles of each layer θ_i, the thickness of each layer, the loads conditions.
2. Calculates the [Q] matrix for each layer.
3. Compute the T matrix for each layer.
4. Calculates the $[\overline{Q}]$ for each layer.
5. Find the location of the top and bottom surface of each layer, $h_k (k = 1\ to\ n)$.
6. Calculate the $[A]$, $[B]$, $[C]$, $[D]$, $[E]$, $[\mathcal{S}_i], i = 1, 2, 3, 4$ matrices.
7. Substitute these matrices as well as the applied loading and solve the fifteen simultaneous equations to determine the mid-plane strains $e_{\alpha\beta}$, the curvature $K_{\alpha\beta}$ and the Gauss curvature $Q_{\alpha\beta}$, the warping tensor $\Upsilon_{\alpha\beta\overline{q}}$, the transverse and normal strain tensors ϕ_1, ϕ_1, ϕ_3.

8. Find the local strains and stresses for each layer.

This algorithm is extended to find also the deflection and fundamental frequencies of the laminated composite shells under transverse loading.

5.1 Analytical analysis using the proposed algorithm

Graphite/epoxy composites has advantages of light weight, high strength, corrosion resistance, low expansion and are often used in the form of composite pressure vessel for various engineering applications. In some tests conducted by Kaw [14], and [3] , the stresses and strains in a graphite/Epoxy composite laminate were examined. Other analytical theory that use this method is available in [9] (see also [12]). This laminate consists of three layers, with fiber angles of 0^o, 30^o and -45^o, and each layer had a thickness of $5mm$. The 2D and 3D material properties, material limits and loading conditions used in this experience are given in Table (1).

Table 1: Table showing the stiffness and strength properties of a 2D graphite/epoxy structure.

Stiffness Properties	E_1**(Gpa)**	E_2**(Gpa)**	ν_{12}	G_{12}**(Gpa)**	
Value	181	10.3	0.28	7.17	
Strength Properties	X_t**(Mpa)**	X_c**(Mpa)**	Y_t**(Mpa)**	Y_c**(Mpa)**	**S(Mpa)**
Value	1500	1500	40	246	68

We present an analytical method as in [9] which gives approach for determining the local stresses and strains in each layer. The results of tests are presented in Table.(2)-(3).

The Table.(3) shows the influence of Gauss tensor in the strain and stress energy in the laminated shell. In some the both analysis give the results practically same. The strains and stress at the top, middle and bottom are well captured. When the shell is thin we retrieve the results obtained by several authors in literature.

5.2 A interlaminar study for a laminated shell.

We use here the same algorithm to perform interlaminar phenomenon in the laminated shell structure. The 3D material properties, material limits and loading conditions used in interlaminar experience are given in Table. 4.

Where X_t and Y_t are the tensile strengths in the fiber and transverse directions and S the shear strength for the composite lamina. By the 3D constitutive relation developed here we can find directly the interlaminar stresses and strains as proposed by [18]. The results of tests are presented in Table 5 and 6.

The Table.(5)-(6) show interlaminar and transverse deformation/stress of the laminate obtained directly by analytical method when the curvature effect is neglected. Here, the nature of stress concentration that occurs in composite laminates that have edge boundaries is captured without solve a 3D elasticity boundary value problem. In addition, the usual through-the-thickness term assumed for the displacements permits to obtain more accurate results. Using our constitutive relation, we are able to determine both interlaminar shear stress and interlaminar normal directly without neglecting deformation in the thickness direction as in [18]. The theory proposed by these authors named Interlaminar Shear Stress Continuity Theory (ISSCT), could not able to calculate interlaminar normal stress directly from the constitutive equations. Our 3D constitutive relation is also able to calculate transverse deformation even when the composite interface is non-rigid without to use the Interlayer Shear Slip Theory (ISST) based on a multilayer approach of [17].

Table 2: Table showing local stresses (Mpa) deviation both of classical LFL and present LFL

		$\sigma_{xx}(10^2)$		$\sigma_{yy}(10^2)$		$\sigma_{xy}(10^2)$	
Layer n°k	**location**	**Anal** [3, 4]	**Present** ABCDE-matrix	**Anal** [3, 4]	**Present** ABCDE-matrix	**Anal** [3, 4]	**Present** ABCDE-matrix
1 (0°)	top	3.351	-2.999	6.188	- 1.949	-2.750	-2.0630
	middle	4.464	2.668	5.359	2.8313	-2.015	-1.688
	bottom	5.577	5.593	4.531	5.535	-1.280	-1.331
2 (30°)	top	9.973	13.86	4.348	5.191	1.890	2.479
	middle	15.023	20.413	3.356	5.554	1.702	3.025
	bottom	20.074	15.732	2.364	4.195	1.513	2.411
3 (−45°)	top	25.86	51.2014	2.123	2.719	-1.638	-3.173
	middle	9.786	14.402	2.010	0.506	-0.995	-0.950
	bottom	-6.285	-41.49	1.898	-3.100	-0.353	2.601

Table 3: Table showing local strains(mm) deviation both of classical LFL and the 2D version of LCE for a moderately thickness shell with very large radius curvature.

		$\epsilon_{xx}(10^-4)$		$\epsilon_{yy}(10^-4)$		$\epsilon_{xy}(10^-4)$	
Layer n°k	**location**	**CLST** [3, 4, 14]	**Present** ABCDE-matrix	**CLST** [3, 4, 14]	**Present** ABCDE-matrix	**CLST** [3, 4, 14]	**Present** ABCDE-matrix
1(0°)	top	8.944	-13.5586	595.5	-184.593	-383.6	-287.73
	middle	16.37	10.365	513.4	270.76	-281.1	-235.431
	bottom	23.80	22.341	431.3	528.81	-178.5	-185.689
2(30°)	top	48.37	68.55	406.7	482.6	263.6	345.77
	middle	77.81	104.18	302.6	507.73	237.4	421.94
	bottom	107.3	80.42	198.5	383.02	211.1	336.31
3(−45°)	top	139.6	278.6	166.1	184.7	-228.4	-442.55
	middle	50.96	78.78	180.0	26.93	-138.8	-132.55
	bottom	-37.66	-224.44	194.0	-236.818	-492.8	362.80

Table 4: Table showing the stiffness and strength properties of a 3D graphite/epoxy structure.

Stiffness Properties	E_1 **(Gpa)**	E_2 **(Gpa)**	E_3 **(Gpa)**	ν_{12}	ν_{13}	ν_{23}	G_{12} **(Gpa)**	G_{13} **(Gpa)**	G_{23} **(Gpa)**
Value	128.484	9.135	9.135	0.249	0.249	0.249	5.705	5.705	3.66
Strength Properties	X_t**(Mpa)**	Y_t**(Mpa)**	**S(Mpa)**						
Value	2266	70	84.11						

5.3 Global and local transverse and plane deformation/stress

The second interlaminar test is done with the symmetric laminated $[45^o/55^o/65^o/75^o]_s$ under transverse load $F = 20KN$. The thickness of thickness of each layer are respectively $h_{45} = 26mm$; $h_{55} = 0.65mm$; $h_{65} = 1.95mm$; $h_{75} = 1.3mm$. The material used here is the verre/epoxy and the characteristic of these material can be found in [4]. The global and local deformations and stresses are assessed in each layer. The solution of this test is computed via the simple algorithm and are presented in Figs.(4)-(6).

Table 5: Matlab solution showing local 3D stresses (Mpa)(interlaminar stresses) using directly three-dimensional Laminated Fundamental Law

Layer n°k	**Position**	$\sigma_{xx}(10^4)$	$\sigma_{yy}(10^4)$	$\sigma_{zz}(10^4)$	$\sigma_{xz}(10^4)$	$\sigma_{yz}(10^4)$	$\sigma_{xy}(10^4)$
1(0°)	top	2.2098	0.1881	0.5974	-0.0001	-0.0002	-0.0036
	middle	1.6329	0.1452	0.4431	-0.0001	-0.0001	-0.0020
	bottom	1.0237	0.0964	0.2792	-0.0000	-0.0001	-0.0007
2(30°)	top	-0.17380	-0.00210	-0.04347	-0.00001	-0.00007	0.00033
	middle	-0.12111	0.00012	-0.02980	0	0	0.00205
	bottom	-0.01739	0.00319	-0.00320	0.00001	0.00007	0.00276
3(−45°)	top	-0.5118	-0.0375	-0.1364	0.0000	0	-0.0039
	middle	-1.0576	-0.0911	-0.2857	0.0001	0	-0.0006
	bottom	-1.5268	-0.1419	-0.4152	0.0001	0	0.0048

Table 6: Matlab solution showing local 3D strains(mm) using three-dimensional LCE given by Eq.(45)

Layer n°k	**Position**	ϵ_{xx}	ϵ_{yy}	ϵ_{zz}	ϵ_{xz}	ϵ_{yz}	ϵ_{xy}
1 (0°)	top	0.0056	0.0002	0.0004	-0.0003	-0.0003	-0.0063
	middle	0.0036	0.0065	0.0004	-0.0002	-0.0002	-0.0034
	bottom	0.0017	0.0095	0.0004	-0.0001	-0.0001	-0.0011
2 (30°)	top	0.0032	0.0076	0.0004	-0.0000	-0.0001	0.0062
	middle	0.0027	0.0069	0.0004	0	0	0.0082
	bottom	0.0012	0.0038	0.0004	0.0000	0.0001	0.0069
3 (−45°)	top	0.0011	0.0021	0.0004	0.0001	0	-0.0068
	middle	-0.0034	-0.0021	0.0004	0.0003	0	-0.0010
	bottom	-0.0093	-0.0078	0.0004	0.0004	0	0.0084

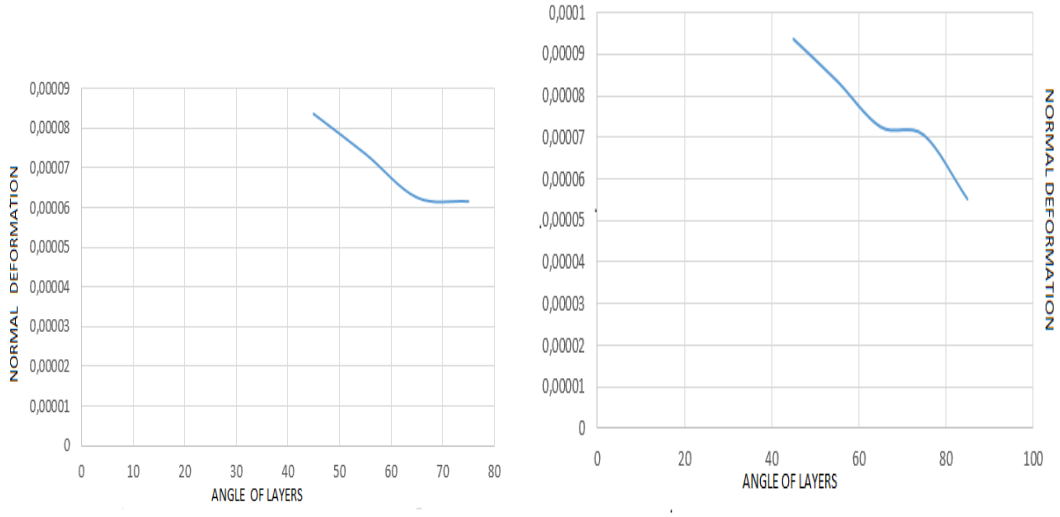

Figure 4: normal deformations, left local, right global.

Figs.(4)-(6) show the variation through the thickness of the 3D laminated shell. Our analysis is able

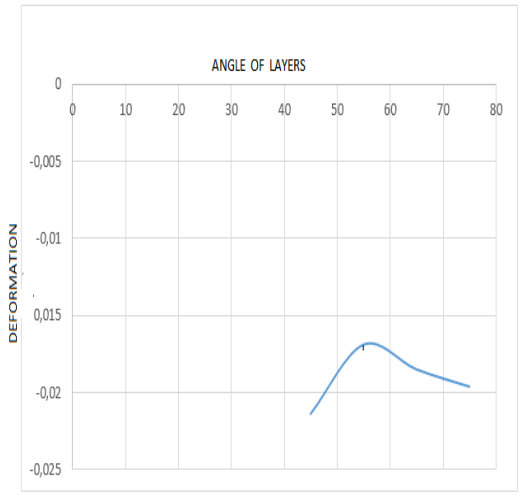

Figure 5: Numerical solution, global plane deformations

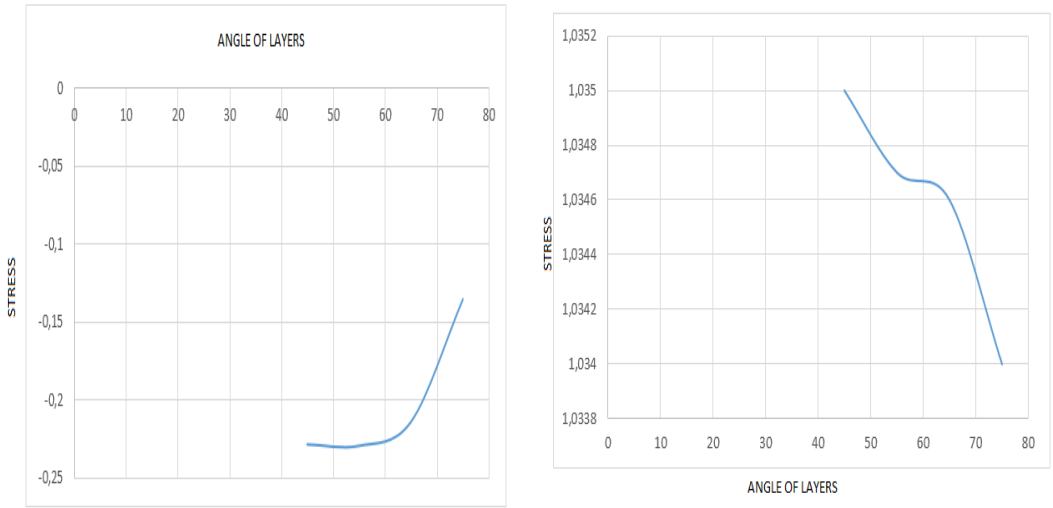

Figure 6: Numerical solution. Left, Global plane stresses and right, local normal stress.

to reproduce entirely the behavior the shell accounting all the mechanical couplings which appear during the deformation. This study is essential for preliminaries design to reduce the effort of calculation and the experimental dispenses. Such studies can help to solve some analysis of LCS (symmetric, anti-symmetric, etc.) without major modifications. The use of simple algorithm above can be crucial for the future investigations.

5.4 Free vibration analysis

For natural vibration analysis, all applied loads are set to zero $\{F(t)\} = \{0\}$ and we assume that the periodic solutions in Eq. (65) are of the form:

$$\begin{aligned} U_{nm}(t) &= U^0_{nm}e^{i\mathbf{w}t}; \quad V_{nm}(t) = V^0_{nm}e^{i\mathbf{w}t}; \quad W_{nm}(t) = W^0_{nm}e^{i\mathbf{w}t}; \overline{Q}_{nm}(t) = \overline{Q}^0_{nm}e^{i\mathbf{w}t}; \\ \theta_{1mn} &= \theta^0_{1mn}e^{i\mathbf{w}t}, \theta_{2mn} = \theta^0_{2mn}e^{i\mathbf{w}t}, \\ \Phi_{1mn} &= \Phi^0_{1mn}e^{i\mathbf{w}t}, \Phi_{2mn} = \Phi^0_{2mn}e^{i\mathbf{w}t}, \end{aligned} \tag{70}$$

where i is the imaginary unit, $i^2 = -1$; $\mathbf{w}$ is natural frequency. In addition, substituting Eq. (65) into Eq. (67), it can be obtained the equation:

$$([K] - \mathbf{w}^2[M])\{\overline{\Delta}\} = \{0\}, \tag{71}$$

where $\overline{\Delta} = \{U^0_{nm},\ V^0_{nm},\ W^0_{nm},\ \overline{Q}^0_{nm},\ \theta^0_{1mn},\ \theta^0_{2mn},\ \Phi^0_{1mn},\ \Phi^0_{2mn}\}^t$.
For a non-trivial solution, the determinant of the coefficient matrix of Eq. (71) should be zero. Solving the resulted determinant, we get the natural frequency, $\mathbf{w}_{mn}$, corresponding to mode (m, n). In this test, the frequencies in Hz are evaluated in the laminated for several thickness ratio and presented in Table (7). The cylindrical shell is constituted of three layers (90/0/90) and four layers composite cross-ply (90/0/90/0). Each layer has same thickness $h_k = h/Nb$, where Nb is the number of layers. The material composite for both layered structures have Young modulii $E_1 = 132.38Gpa$, $E_2 = E_3 = 10.756Gpa$ shear modulii $G_{12} = G_{13} = 5.6537Gpa$ $G_{23} = 3.603Gpa$, poisson ratios are $\nu_{12} = \nu_{13} = 0.24$ and $\nu_{23} = 0.49$ and mass density $\rho = 1600Kg/m^3$. The results of these tests are presented in Table. (7).

Table 7: Frequencies in Hz for the simply supported cross-ply laminated composite cylindrical shell panels. Validation with literature result

	Layers	**90/0/90/0**		**90/0/90**	
$\frac{R}{h}$	(m,n)	[Present]	[35]	[Present]	[35]
1000	(2,1)	5.353	5.353	5.634	5.634
	(5,1)	6.491	6.491	3.435	3.435
	(4,1)	4.395	4.395	4.395	2.752
100	(2,1)	11.24	11.24	7.717	7.717
	(1,1)	13.208	13.20	13.431	13.43
	(3,3)	28.107	28.10	21.627	21.62
10	(1,1)	25.203	25.20	20.814	20.81
	(2,1)	77.144	77.58	49.298	49.51
	(2,3)	100.08	100.6	93.274	93.94
5	(1,1)	37.54	38.63	31.25	33.17
	(2,1)	105.45	107.5	86.21	88.55
	(2,3)	137.45	138.0	130.24	132.9

Discussion

The results shown in Tab. (7) indicate clearly that the convergence is obtained when the thickness-ratio is small than 1/10 and with the increase of number of layers, the frequencies increase. The presence of some mechanical couplings in the 3D LCE influence the damping of the laminated shell. This may be explained by the fact that the number of shell layers is increased, the laminate becomes thicker and becomes stiffer. This creates a strong resistance to the deformation (the vibration). The period of vibration becomes smallest due to the presence of some mechanical couplings that influence the dynamic of the laminated (by

Table 8: Non-dimensional deflection for cross-ply laminated composite cylindrical shells under transverse load.

	0/90/0			**0/90**		
$\frac{R}{h}$	[Present]	[29]	[33]	[Present]	[29]	[33]
2	1.387	1.436	1.439	1.978	2.079	2.088
4	0.412	0.457	0.457	0.842	0.854	0.857
10	0.142	0.144	0.143	0.491	0.493	0.494
50	0.0798	0.08	0.081	0.409	0.409	0.409
100	0.078	0.078	0.078	0.403	0.403	0.404
500	0.077	0.077	0.077	0.399	0.399	0.398

damping the effects of vibration) while increasing their frequency (Hz). It clearly showed how the extensional-twisting-shear, extensional-Gauss bending-shearing, Gauss bending-shearing influenced the center deflection and fundamental frequencies of LCS when the ratio-thickness $\chi = \dfrac{h}{2R}$ becomes greater.

5.5 Variation through-the-thickness

Here, the variation through-the-thickness (transverse displacement) with different thickness ratio for two cylindrical laminates: bi-directional (0/90) antisymmetric and symmetric cross-ply (0/90/0). Each layer is an orthotropic material and has cylindrical anisotropy. Here the layers have the same thickness and the laminate is subjected to a transverse load $q(\theta) = \sum_{n=0}^{\infty} q_n \sin(p\theta)$ (uniformly distributed $q_n = \dfrac{2q_0}{n\pi}$) on the top surface. The parameters of the cylindrical shell are: radius $R_0 = 10$, $h =$. The plane-polar coordinates are considered such that the radius vary through the thickness. The normalized result of transverse displacement (deflection) $\overline{w} = \dfrac{10E_2}{q_0 h \chi}$, $\chi = \dfrac{R}{h}$. We compare the results of deflection using elasticity solution based on stress function approach of [29] and displacement-based approach of [33] with the results obtained by using the proposed Navier based method (via our 3D constitutive relation given by (45)) are presented in Table (8) for two lamination schemes.

When the laminated become thicker, the deflection results obtained by our method are highly different than of those presented by [29] and [33] due to contribution of warping and Gauss deformation tensors that increase. When the thickness of the shell become smaller, the CLST, FSD based models and our models give the same exact solutions. In fact, thin shells neglect the effect of the above tensors due to variation in the thickness. The tensors $q\Upsilon_{\alpha\beta}$, $Q_{\alpha\beta}$ and $\partial_\alpha \overline{q}$ disappear.

6 Concluding remarks

In this paper, we have firstly proposed a new 3D exact laminated shell model to analyze the static and dynamic mechanical behavior of LCS. Second, we proposed some 2D and 3D exact analysis of different laminated shell and plates configurations. Using Hamilton's principle and a new three-dimensional constitutive equations (obtained via a original 2D shell kinematics with through-the-thickness variable), one has derived a new original motion equation of the laminated shells. This equation of motion is more general than that obtained previously by the same authors and include some mechanical couplings appearing only in the movement of 3D laminated shells subjected to a transverse load applied at the top in nonharmonic and harmonic form. These couplings do not appear when we use directly elasticity theory or the method based on the three-dimensional shell equilibrium equations developed in a general orthogonal curvilinear reference system. Such methods is not able to reproduce well a mechanical behavior of laminated shell under twisting load and when the warping section become important. Some Benchmarks were performed to show the performance

of the 3D exact model. Advantages of these new mathematical modelings are the presence of other 3D laminate stiffness coefficients which improves the prediction of displacement, force and moment resultants significantly. The present mathematical modelings of the static and dynamic behavior of laminated shells (cylindrical, spherical, cone, arch, etc.) should serve as a reference for future investigations.

Conflict of Interests

The authors declare that there is no conflict of interests regarding the publication of this paper.

Acknowledgements

This work is under the project sanctioned by the laboratory of energy modeling materials and methods (E3M), National Advanced School Polytechnic of Douala of University of Douala-Cameroon.

References

[1] S. A. Ambartsumyan, "A refined theory of anisotropic shells," FTD-MT-24-1699-71, Ohio, 1969.

[2] S. A. Ambartsumyan, " theory of anisotropic shells," Moscou (1961),English translation, NASA, TTF-118, May 1964.

[3] A. Ramsaroop and K. Krishnan. Using Matlab to design and analyse composite Laminates. Engineering, 2 (2012), pp. 904-916.

[4] J. Berthelot, "Mécanique des matériaux et structures composites,"IMANS france 1993.

[5] Salvatore Brischetto. Exact three-dimensional static analysis of single and multilayered plates and shells. Composite Part B (2017), pp.

[6] S. Brischetto, Three-dimensional exact free vibration analysis of spherical, cylindrical, and flat one-layered panels, Shock and Vibration, vol.2014, 1-29, 2014.

[7] S. Brischetto, An exact 3D solution for free vibrations of multilayered cross-ply composite and sandwich plates and shells, International Journal of Applied Mechanics, 6, 1-42, 2014

[8] E. Carrera, A. Pagani, S. Valvano. Shell elements with through-the-thickness variable kinematic for the analysis of laminated composite and sandwich structures. Composite Part B (2017), pp.

[9] Erik Estivalezes and Jean-Jacques Barrau. Analytical theory for an approach calculation of composite box beams subjected to tension and bending. Composites Part B 29B (1998) 371-376.

[10] A. G. Feumo, R. Nzengwa and A. J. Nkongho, "Finite element model for elasic thick shells using gradient recorvery method," Mathematical problem in engineering,Vol 2017,Hindawi.

[11] B. Gasemzadeh, R. Azarafza, Y. Sahebi and A. Motallebi, Analysis of free vibration of cylindrical shells on the basis of three dimensional exact elasticity theory, Indian Journal of Science and Technology, 5, 3260-3262, 2012.

[12] P.V. Gopal Krishna, Podila Meghana, A.Sai Kumar and K. Kishore,"Design and Analysis of Carbon Fiber Reinforced Composite Shell Structure Using Classical Laminate Plate Theory",British Journal of Applied Science and Technol

[13] T. Kant, K. Swaminathan, "Estimation of transverse/interlaminar stresses in laminated composites - a selective review and survey of current developments", Composite Structures 49(2000), pp. 65-75.

[14] A. K. Kaw. Mechanics of Composite Materials. CRC Press LLC, Boca Raton, 1997.

[15] Lee C-Y, Liu D.," An interlaminar stress continuity theory for laminated composite analysis", Computer and Structure 1992, 42(1)pp. 69-78.

[16] C.T. Loy and K.Y. Lam, Vibration of thick cylindrical shells on the basis of three-dimensional theory of elasticity, Journal of Sound and Vibration, 226, 719-737, 1999.

[17] Lu X, Liu D., "An interlaminar shear stress continuity theory", In: Proceedings of the Fifth Technical Conference of the American Society for Composites. Lancaster PA: Technomic, 1990:479-83

[18] Lu X, Liu D."Interlayer shear slip theory for cross-ply laminates with nonrigid interfaces", AIAA J 1992;30(4):1063-73.

[19] Quaresimin, Luca Susmel, Ramesh Talreja. Fatigue Behavior and life assessment of composite laminates under multiaxial loadings. International Journal of fatigue, 32 (2010) 2-16.

[20] Arno Ngatcha, "Formulation of laminated composite shell for Marine application," Master's thesis, Faculty of Industrial Engineering, University of Douala, Cameroon, April 2019, Technical report resaearch.

[21] Ngatcha Ndengna Arno Roland , Renaud Ngouanom, Edmon Mbangue and Pandong Achille. Two dimensional static mechanic analysis of laminated composite tube using ABCDE matriix with no correction factor, International Journal of Mechanic 2021, 1(15), 107-120. DOI:10.46300/9104.2021.15.12

[22] Ngatcha N. Arno Rroland , R. Ngouanom. G. Joel and A. Pandong, (2022) " A Two-Dimensional Model to Analyze the Static and Dynamic Mechanical Behavior of Multilayered shell Structures.," Composite Structures, 295(4), 115754. https://doi.org/10.1016/j.compstruct.2022.115754.

[23] Mbangue Nzengwa Ekmon, Ngatcha Ndengna Arno Roland, Joel Renaud Ngouanom Gnidakouong,Joseph Nkongho Anyi and Robert Nzengwa. 3D exact static analysis of anisotropic shells: case of uniform cylinder composite tube. To appear in Computer and concrete, 2023.

[24] A. J. Nkongho,J. C. Amba, Dieudonné Essola, A. C. V. Ngayihi,"Generalised assumed strain curved shell finite elements(CSFE-sh) with shifted-Lagrange and applications on N-T's shells theory," Curved and layer. Struct. 2020; (7) 125-138.

[25] R. Nzengwa,and S. B. H. Tagne. A two-dimensional model for linear elastic thick shells. International journal of solid and structures **36**(1999), pp. 5141-5176

[26] R. Nzengwa,"A 2D model for dynamics of linear elastic thick shell with transversal strains variation proceeding of 8th conference on dynamical systems and applications," Lódź, Poland (2005)December 12-15.

[27] J. N. Reddy,"Mechanics of laminated composite plates and shells.Theory and analysis," Journal composite materials, Vol. 5, CRC press Second edition, 2004.

[28] J.G. Ren, Exact solutions for laminated cylindrical shells in cylindrical bending, Composite Science and Technology, 29, 169-187, 1987.

[29] J.G. Ren, Analysis of simply-supported laminated circular cylindrical shell roofs, Compos. Struct. 11 (1989) 277-292, https://doi.org/10.1016/0263-8223(89) 90092-5.

[30] T.K. Varadan and K. Bhaskar, Bending of laminated orthotropic cylindrical shells - an elasticity approach, Composite Structures, 17, 141-156, 1991.

[31] S.S. Sahoo, C.K. Hirwani, S.K. Panda and D. Sen, "Numerical analysis of vibration and transient behaviour of laminated composite curved shallow shell structure: An experimental validation", Scientia Iranica B (2018) 25(4), 2218-2232.

[32] Y. Stavsky, "Bending and Stretching of Laminated Anisotropic Plates," ASCE, Journal of the Engineering Mechanics Division, vol.87, n°16, p.31, 1961.

[33] Sharvari N. Dhepe, Abhay N. Bambole, Yuwaraj M. Ghugal. An elasticity solution of laminated cylindrical panel. Force in Mechanics 2022, (9) 100147.

[34] M. Tahani, A. Andakshideh, S. Maleti. Interlaminar stresses in thick cylindrical shell with arbitrary laminations and boundary conditions under transverse loads. Composites Part B (2016) 151-165.

[35] F. Tornabene, S. Brischetto, N. Fantuzzi and E. Viola, Numerical and exact models for free vibration analysis of cylindrical and spherical shell panels, Composites part B: engineering, 81, 231-250, 2015.

[36] W Zaki,V Nguyen and R Umer "A model for inter-laminar shear stress in laminated composites", IOP Conf. Series: Journal of Physics: Conf.Series 814(2017) 012006.